ASTRON

Netherlands Institute for Radio Astronomy

Introduction to Low-Frequency Radio Astronomy

- John McKean
- (ASTRON and Kapteyn Astronomical Institute)

Preamble

- **AIM:** This lecture aims to give a general introduction to low frequency radio astronomy, focusing on the issues that you must consider and the differences with observations with other telescopes.

- **OUTLINE:**

1. The radio sky and historical developments
2. The response of a dipole antenna
3. The response of an interferometer
4. Low frequency radio telescopes

1.1 The Radio Window

- Radio Astronomy is the study of radiation from celestial sources at frequencies between $\nu \sim$ 10 MHz to 1 THz (10^7 Hz to 10^{12} Hz).

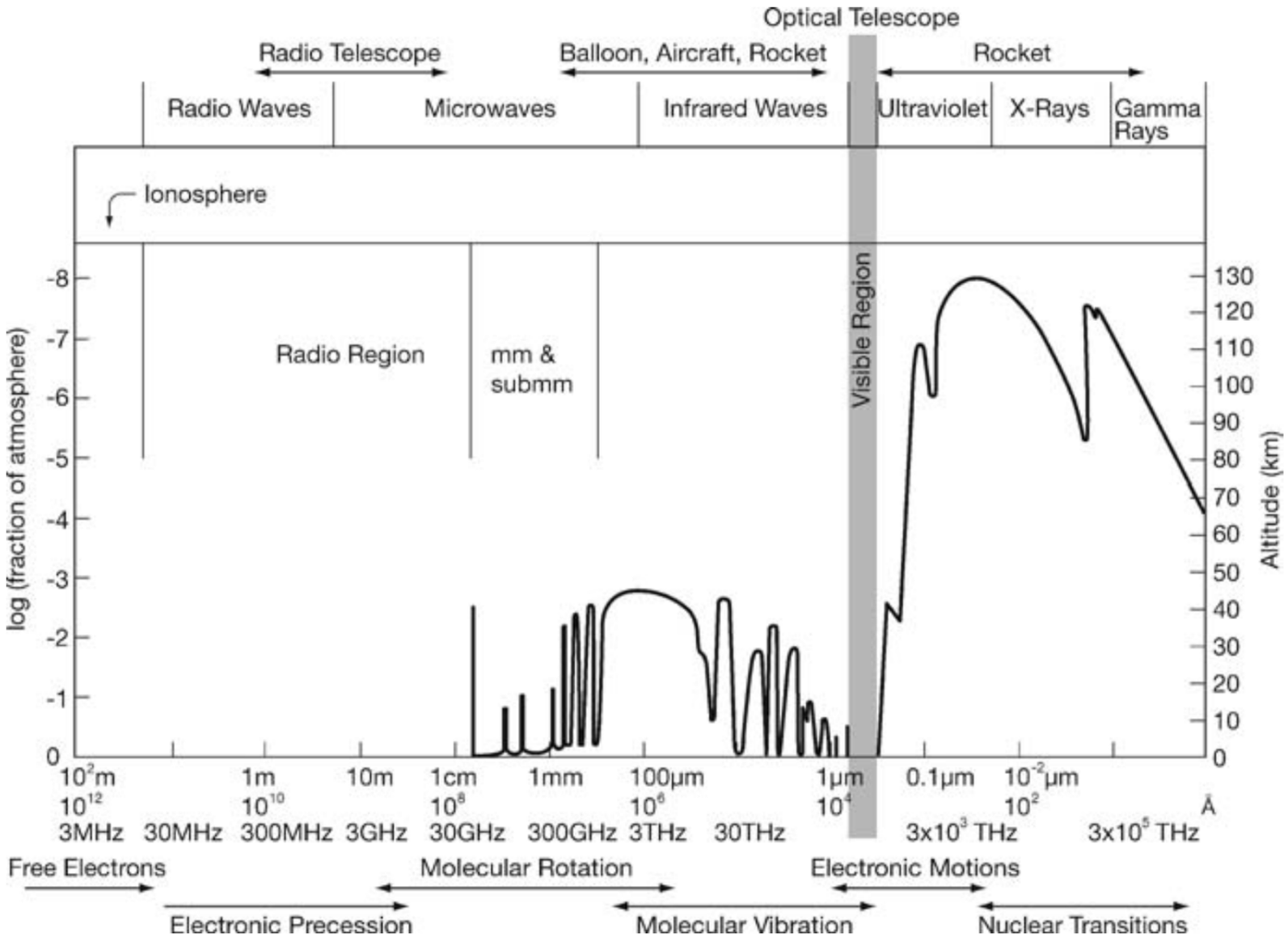

1.1 The Radio Window

- Radio Astronomy is the study of radiation from celestial sources at frequencies between $\nu \sim$ 10 MHz to 1 THz (10^7 Hz to 10^{12} Hz).

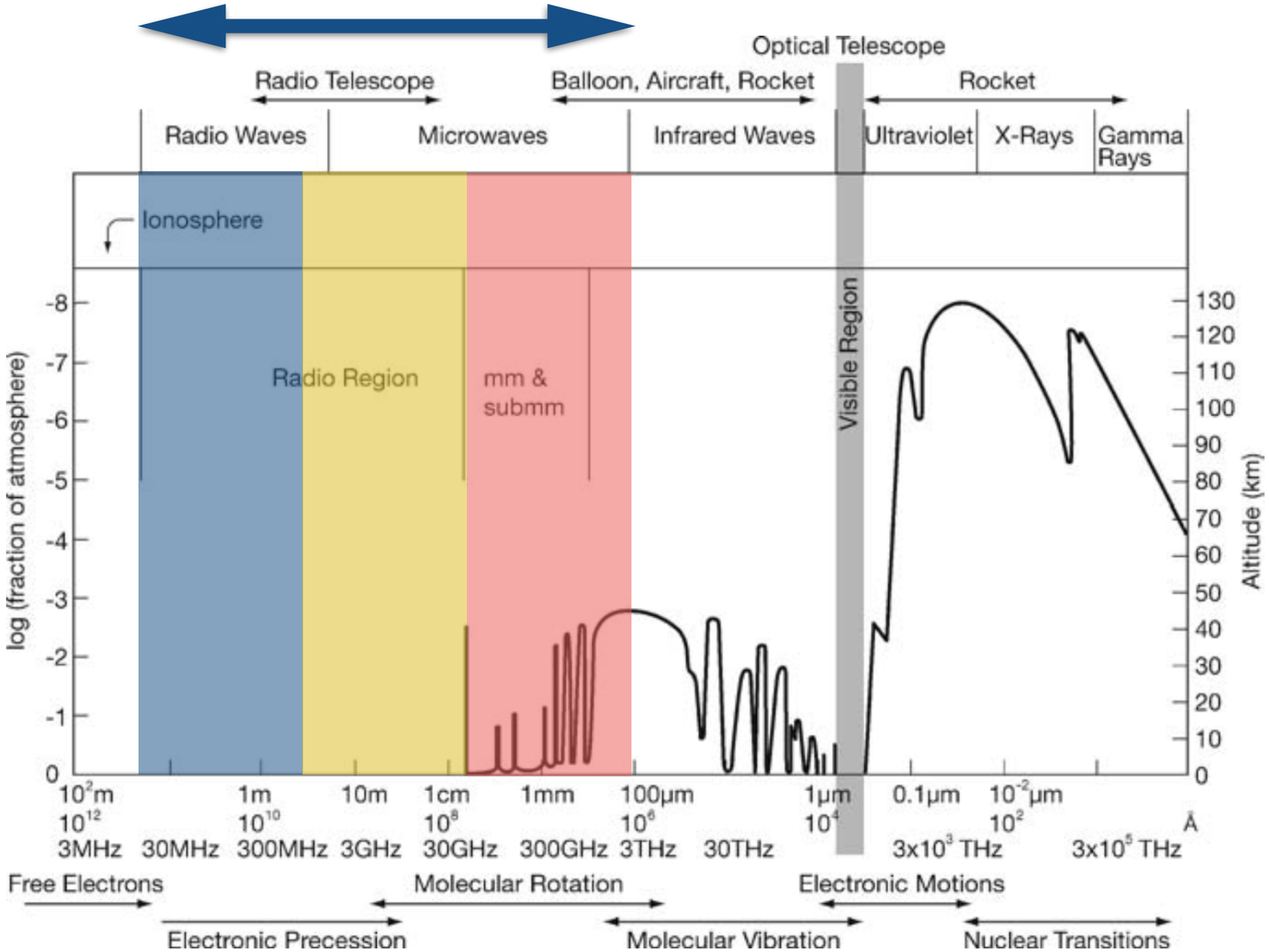

- The observing window is constrained by atmospheric absorption / emission and refraction.
  1) Charged particles in the ionosphere reflects radio waves back into space at < 10 MHz.
  2) Vibrational transitions of molecules have similar energy to infra-red photons and absorb the radiation at > 1 GHz (completely by ~300 GHz).

1.2 The low-frequency cut-off

- The ionosphere consists of a plasma of charged particles (conducting layers), that has an effective refractive index of,

$$n^2 = 1 - \frac{\omega_{\rm p}^2}{\omega^2} = 1 - \left(\frac{\lambda}{\lambda_{\rm p}}\right)^2$$

where, the plasma frequency is defined as,

$$\nu_{\rm p}[{\rm Hz}] = \frac{\omega_{\rm p}}{2\pi} = \left(\frac{N_{\rm e}e^2}{4\pi^2\epsilon_0 m}\right)^{1/2} = 8.97\times10^3\sqrt{\frac{N_e}{[{\rm cm}^{-3}]}}$$

[see Calibration & Ionospheric lectures]

when $\omega < \omega_{\rm p}$, there is no propagation, i.e. total reflection.

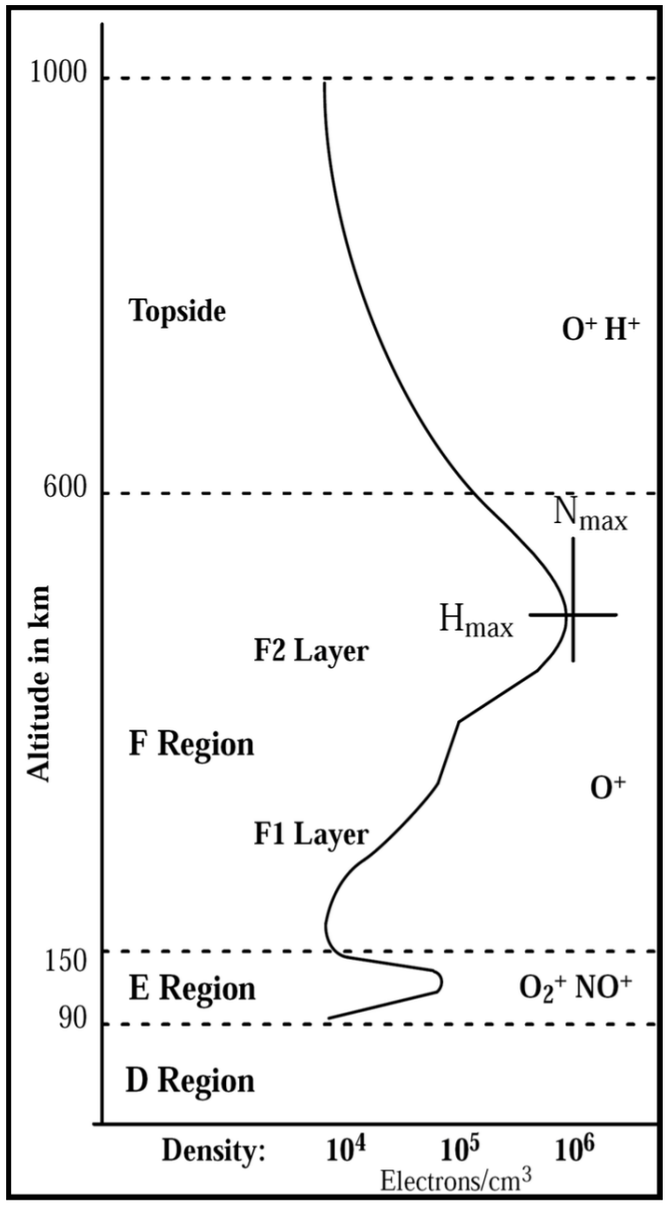

Worked example: What is the cut-off frequency for LOFAR observations carried out when the electron density is $N_e = 2.5 \times 10^5$ cm^{-3} (night time) and $N_e = 1.5 \times 10^6$ cm^{-3} (day time)?

- At frequencies,
  1. $\omega < \omega_p$: n^2 is negative, reflection ($\nu < 10$ MHz),
  2. $\omega > \omega_p$: n^2 is positive, refraction (10 MHz < ν < 10 GHz),
  3. $\omega \gg \omega_p$: n^2 is unity ($\nu > 10$ GHz).

- The observing conditions are dependent on the electron density, i.e. the solar conditions (space weather), since the ionisation is due to the ultra-violet radiation field from the Sun,

$$\mathrm{O}_2 + h\nu \rightarrow \mathrm{O}_2^{+*} + e^-$$

$$\mathrm{O}_2 + h\nu \rightarrow \mathrm{O}^+ + \mathrm{O} + e^-$$

Worked example: What is the cut-off frequency for LOFAR observations carried out when the electron density is $N_e = 2.5 \times 10^5$ cm^{-3} (night time) and $N_e = 1.5 \times 10^6$ cm^{-3} (day time)?

$$\nu_{\rm p}[{\rm Hz}] = 8.97 \times 10^3 \sqrt{\frac{2.5 \times 10^5}{[{\rm cm}^{-3}]}} = 4.5 \text{ MHz} \qquad (\text{night time})$$

$$\nu_{\rm p}[{\rm Hz}] = 8.97 \times 10^3 \sqrt{\frac{1.5 \times 10^6}{[{\rm cm}^{-3}]}} = 11 \text{ MHz} \qquad (\text{day time})$$

- At frequencies,
  1. $\omega < \omega_{\rm p}$: n^2 is negative, reflection ($\nu < 10$ MHz),
  2. $\omega > \omega_{\rm p}$: n^2 is positive, refraction (10 MHz < v < 10 GHz),
  3. $\omega \gg \omega_{\rm p}$: n^2 is unity ($\nu > 10$ GHz).

- The observing conditions are dependent on the electron density, i.e. the solar conditions (space weather), since the ionisation is due to the ultra-violet radiation field from the Sun,

$$\mathrm{O}_2 + h\nu \rightarrow \mathrm{O}_2^{+*} + e^-$$

$$\mathrm{O}_2 + h\nu \rightarrow \mathrm{O}^+ + \mathrm{O} + e^-$$

- Long distance communication developed by Marconi & Ferdinand Braun - Nobel Prize 1909

Evolution of frequency over the years

- pre-1920: <100 kHz.
- ca. 1920: shift to 1.5 MHz.
- post-1920: 10s of MHz (more voice channels, less effected by the ionosphere and thunderstorms).

- Research labs sprung up in early-1900s

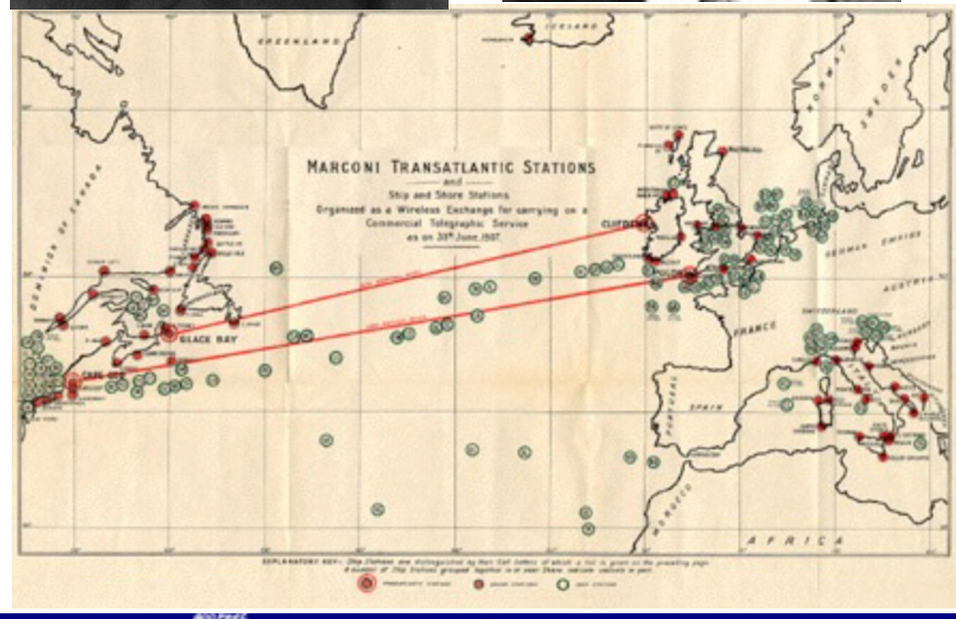

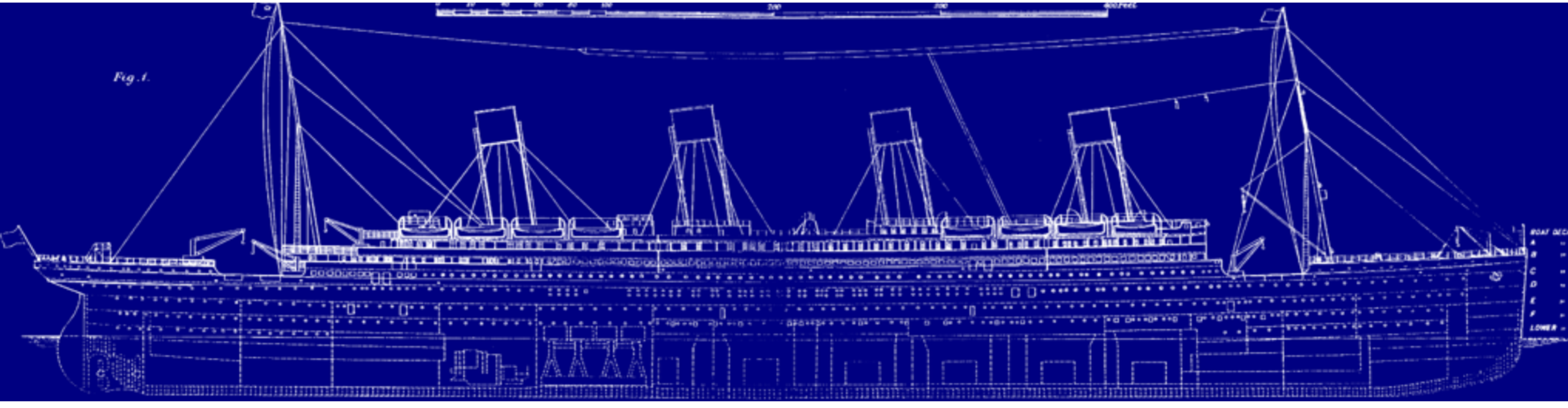

- Karl Jansky (1933, published) discovered a radio signal at 20.5 MHz that varied steady every 23 hours and 56 minutes (Sidereal day).

“The data give for the co-ordinates of the region from which the disturbance comes, a right ascension of 18 hours and declination -10 degrees.” He had detected the Galactic Centre.

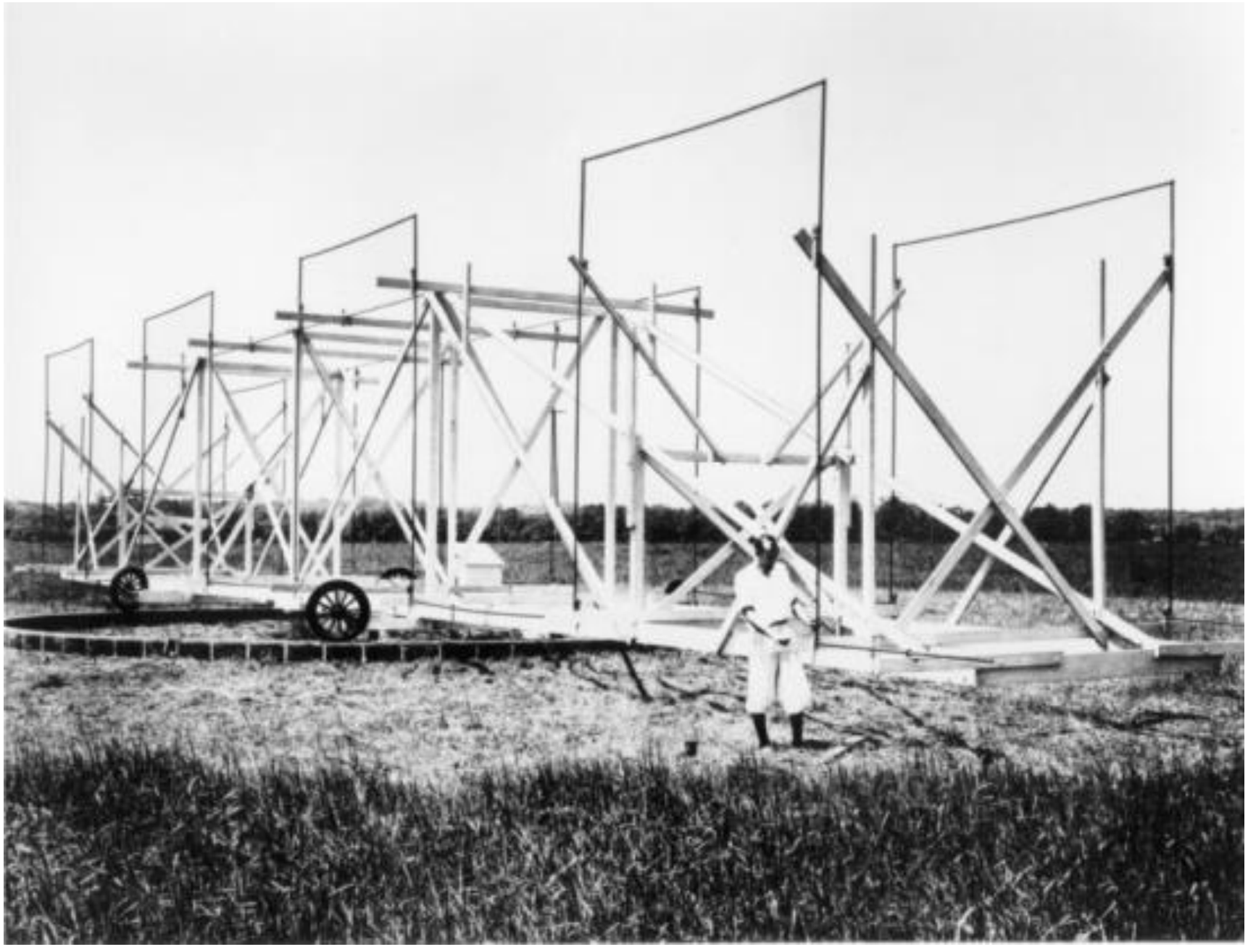

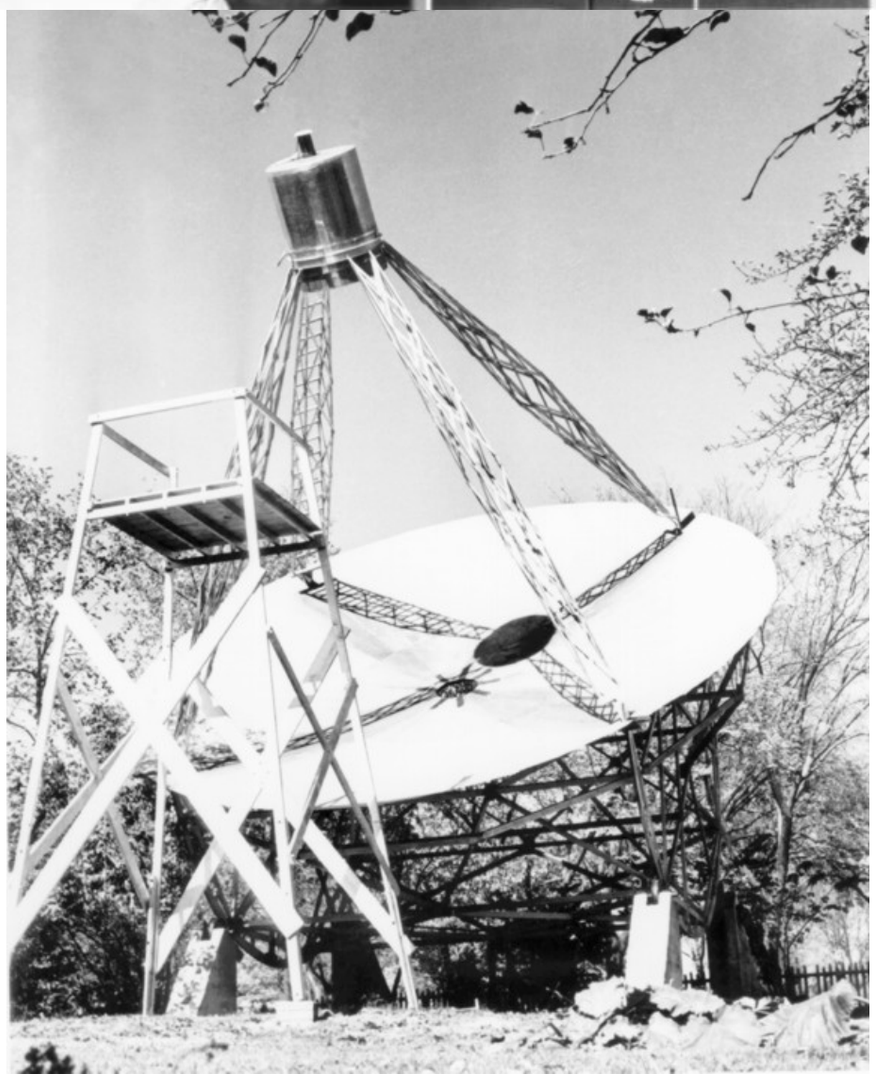

- Grote Reber (1937-39), using his own 10 m telescope, made no detection at 3300 and 910 MHz, ruling out a Planck spectrum (B_ν propto ν^2).

- Detection made at 150 MHz, confirming Jansky's result and finding the spectrum must be non-thermal.

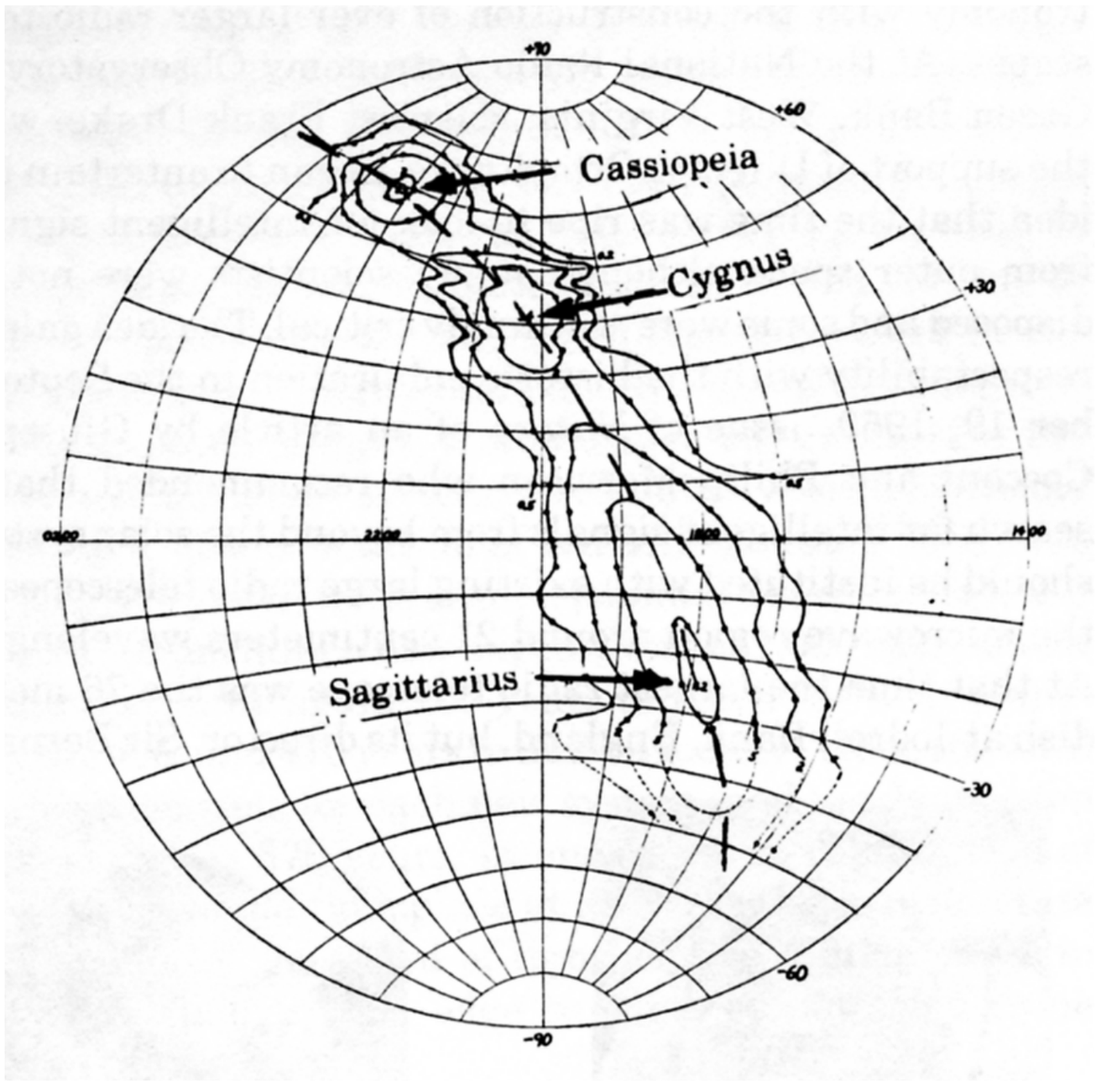

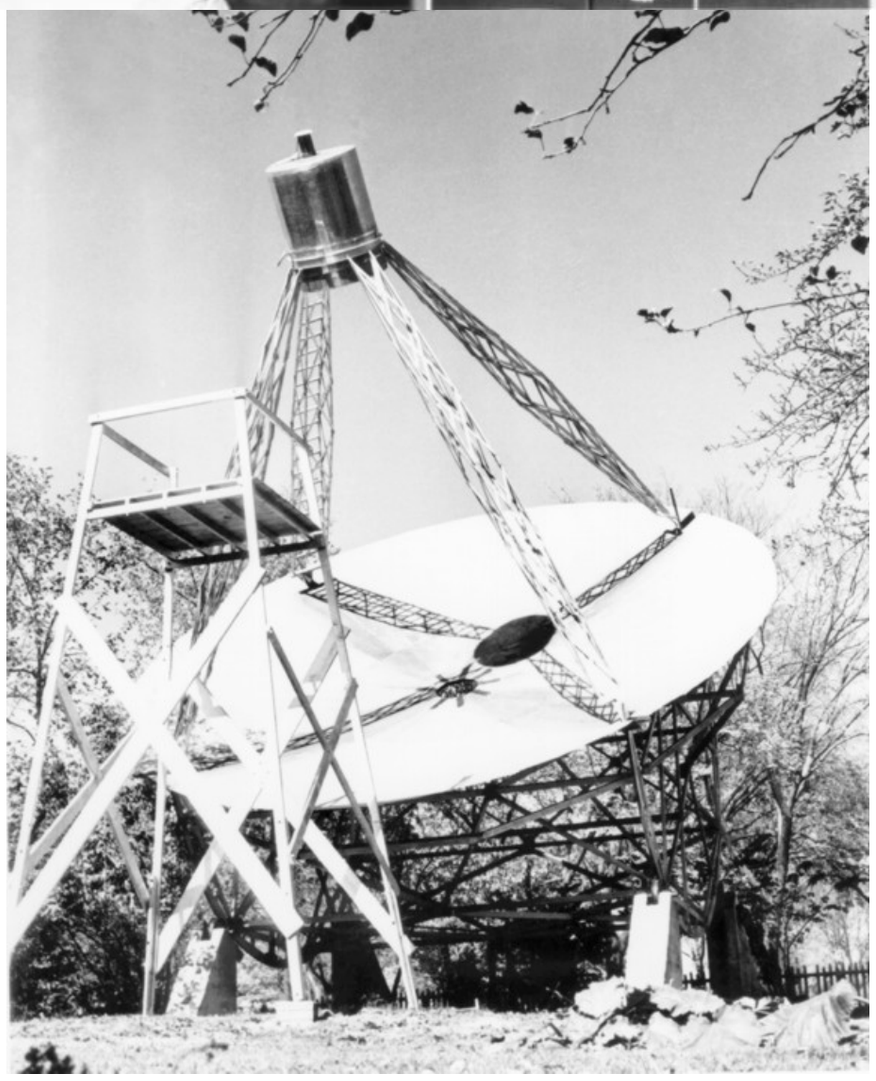

- Grote Reber (1937-39), using his own 10 m telescope, made no detection at 3300 and 910 MHz, ruling out a Planck spectrum (B_ν propto ν^2).

- Detection made at 150 MHz, confirming Jansky's result and finding the spectrum must be non-thermal.

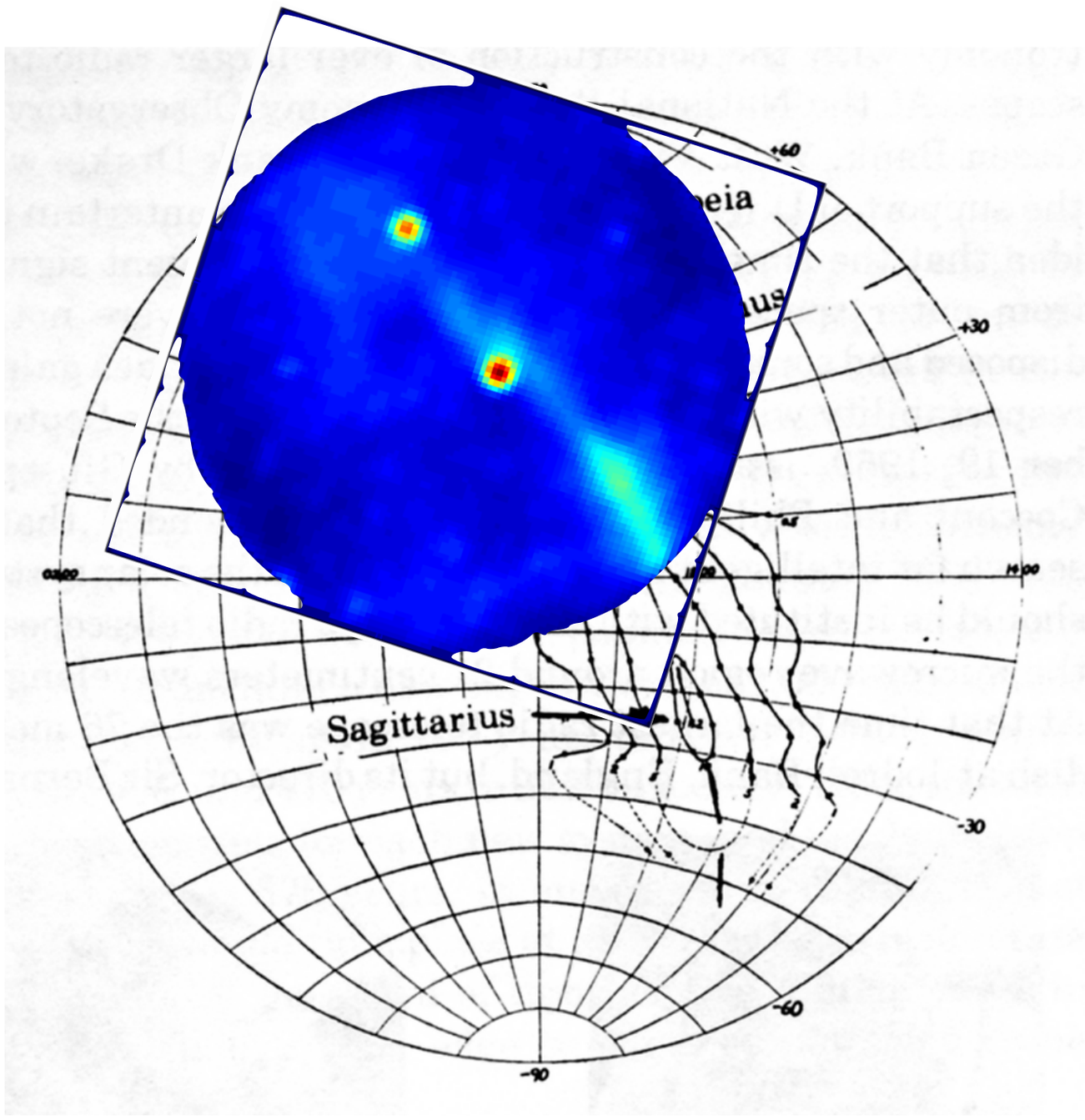

2.1 Dipole antenna fundamentals

- Antenna: A device for converting electromagnetic radiation in space into electrical currents (transmitting and receiving).

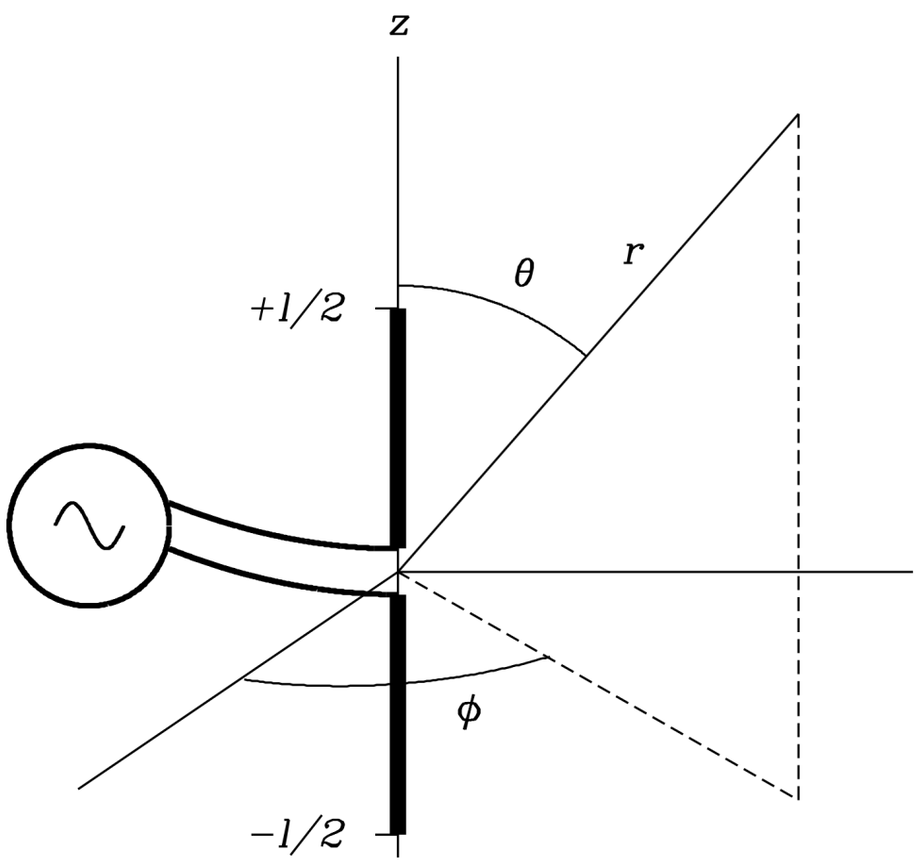

Consider a Hertzian small ($l \ll \lambda$) dipole transmitter (same as for a receiving dipole, but easier to understand).

Two co-linear conductors (e.g. wires, conducting rods), driven by a current source at the gap. The driving current *I* is a time varying sinusoidally with angular frequency,

$$\omega = 2\pi\nu$$

$$I = I_0 \cos(\omega t) = I_0 e^{-i\omega t}$$

(Only consider the real part of $e^{-i\omega t} = \cos(\omega t) + i\sin(\omega t)$)

The time varying current density is defined as, $J = \frac{I}{q} = \frac{I_0}{q} e^{-i\omega t}$ inside the dipole,

and $J = 0$ outside the dipole.

- We want to measure the power radiated from such an antenna, so we calculate,
    1. The electromagnetic vector potential *A,*
    2. The magnetic field induction *B*, and hence the magnetic field intensity *H,*
    3. The electric field intensity *E,*
    4. The Poynting flux *S*,
    5. The total power radiated.

1. The electromagnetic vector potential

The induced magnetic field *B* is related to the vector potential by,

$$\vec{B} = \nabla \times \vec{A}$$

where,

$$\vec{A}(x) = \frac{\mu_0}{4\pi} \int\int\int \vec{J}(x) \frac{e^{ik|x-x'|}}{|x-x'|} d^3x'$$

i.e., the integral of the current density over the volume of the dipole (*dV = q dz*).

The current runs from z = −Δl / 2 and z = +Δl / 2 along the z-axis, thus

$$\vec{J}_x = 0 \quad \text{and} \quad \vec{A}_x = 0$$

$$\vec{J}_y = 0 \quad \text{and} \quad \vec{A}_y = 0$$

only $\vec{J}_z = \frac{I}{q} e^{-i\omega t}$ is non-zero.

Therefore, our vector potential becomes,

$$\vec{A}_z = \frac{\mu_0}{4\pi} \int_{-\Delta l/2}^{+\Delta l/2} \frac{I(z)}{q}\, e^{-i\omega t}\, \frac{e^{ikr}}{r}\, q\, dz$$

$$= \frac{\mu_0}{4\pi}\, \frac{e^{-i(\omega t - kr)}}{r} \int_{-\Delta l/2}^{+\Delta l/2} I(z)\, dz$$

If the current is constant,

$$\int_{-\Delta l/2}^{+\Delta l/2} I(z)\, dz = I\, [z]_{-\Delta l/2}^{+\Delta l/2} = I\, \Delta l$$

Therefore, our vector potential for a constant current is,

$$\vec{A}_z = \frac{\mu_0}{4\pi}\, \frac{e^{-i(\omega t - kr)}}{r}\, I \Delta l$$

2. The magnetic induction is related to the magnetic vector potential via,

$$\vec{B} = \nabla \times \vec{A}$$

We can de-compose the curl of A into three orthogonal cylindrical co-ordinates (ρ, ψ, z), using standard definitions,

$$(\nabla \times \vec{A})_\rho = \frac{1}{\rho}\frac{\partial A_z}{\partial \psi} - \frac{\partial A_\psi}{\partial z}$$

$$(\nabla \times \vec{A})_\psi = \frac{\partial A_\rho}{\partial z} - \frac{\partial A_z}{\partial \rho}$$

$$(\nabla \times \vec{A})_z = \frac{1}{\rho}\left(\frac{\partial(\rho A_\psi)}{\partial \rho} - \frac{\partial A_\rho}{\partial \psi}\right)$$

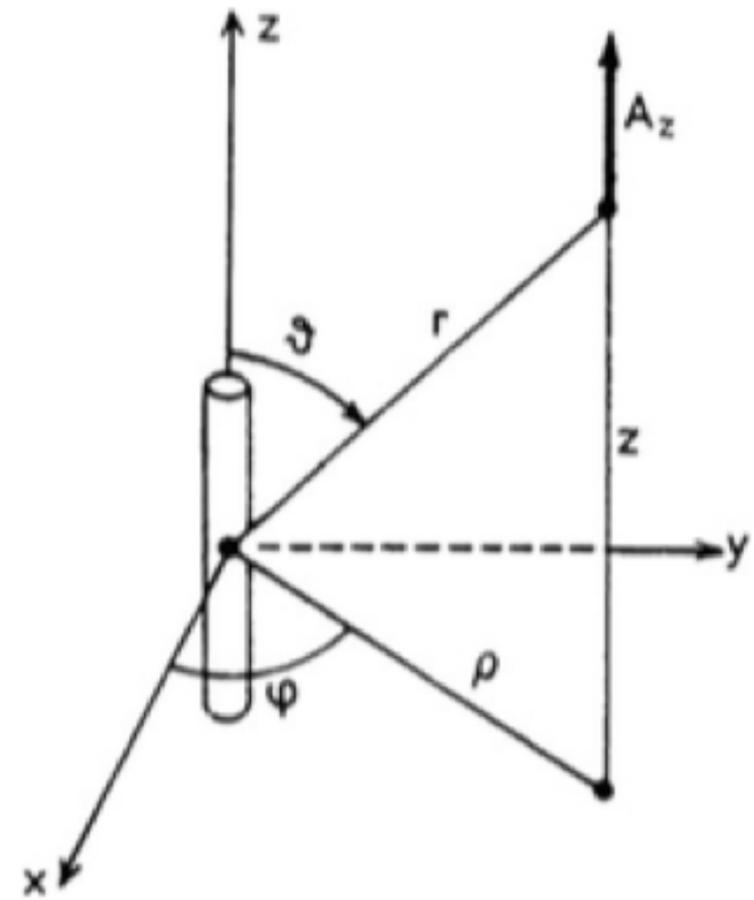

As $A_\rho = A_\psi = 0$, the B-field must be perpendicular to the vector potential (A_z).

For simplicity lets evaluate,

$$B_\psi = (\nabla \times \vec{A})_\psi = \frac{\partial A_\rho}{\partial z} - \frac{\partial A_z}{\partial \rho} = -\frac{\partial A_z}{\partial \rho} = -\frac{\partial A_z}{\partial r}\frac{\partial r}{\partial \rho}$$

In the cylindrical system,

$$r^2 = \rho^2 + z^2 \qquad r = (\rho^2 + z^2)^{1/2}$$

$$\frac{\partial r}{\partial \rho} = \frac{1}{2}(\rho^2 + z^2)^{-1/2}\, 2\rho = \frac{\rho}{r} = \sin\theta$$

Next,

$$\frac{\partial A_z}{\partial r} = \frac{\mu_0}{4\pi} I \Delta l \, e^{-i\omega t} \frac{\partial}{\partial r}\left[\frac{e^{ikr}}{r}\right]$$

We solve this using the quotient rule,

$$\left[\frac{u(r)}{v(r)}\right] = \frac{u'(r)v(r) - v'(r)u(r)}{v(r)^2} \qquad \begin{aligned} u(r) &= e^{ikr} & v(r) &= r \\ u'(r) &= ik\, e^{ikr} & v'(r) &= 1 \end{aligned}$$

$$\frac{\partial}{\partial r}\left[\frac{e^{ikr}}{r}\right] = \frac{ik\, e^{ikr} \cdot r - 1 \cdot e^{ikr}}{r^2} = \frac{(ikr-1)e^{ikr}}{r^2}$$

Therefore our *B*-field in the ψ direction becomes,

$$B_\psi = -\frac{\partial A_z}{\partial r}\frac{\partial r}{\partial \rho} = -i\, k\, \frac{\mu_0}{4\pi} I \Delta l \, \frac{\sin\theta}{r}\left(1 - \frac{1}{ikr}\right) e^{-i(\omega t - kr)}$$

Since,

$$k = \frac{2\pi}{\lambda}$$

$$B_\psi = -i\, \mu_0 \, \frac{I\Delta l}{2\lambda} \, \frac{\sin\theta}{r}\left(1 - \frac{1}{ikr}\right) e^{-i(\omega t - kr)}$$

which, from the materials equations, gives for the magnetic field intensity,

$$B = \mu_0 H \qquad\qquad H_\psi = -i\,\frac{I\Delta l}{2\lambda}\,\frac{\sin\theta}{r}\left(1 - \frac{1}{ikr}\right)e^{-i(\omega t - kr)}$$

Again, the magnetic field intensity is perpendicular to the vector potential, that is, perpendicular to the element.

3. Now, let's consider the electric field intensity. From Maxwell's equations,

$$\nabla \times \vec{H} = \vec{J} + \epsilon_0 \frac{\partial \vec{E}}{\partial t}$$

which, because we are away from the current element (J = 0), simplifies to,

$$\nabla \times \vec{H} = \epsilon_0 \frac{\partial \vec{E}}{\partial t}$$

We are dealing with harmonic waves of the form,

$$E(r,t) = E_0 e^{-i(wt-kr)}$$
$$\dot{E}(r,t) = E_0 e^{-i(wt-kr)} \cdot -i\omega = -i\omega E(r,t)$$

Therefore,

$$E = -\frac{1}{i\omega\epsilon_0}\nabla \times \vec{H}$$

To evaluate E, we must determine the curl of *H*, but as in the case of the B-field, only the H_ψ terms have non-zero entries.

From spherical co-ordinates, the only relevant term of the curl of *H* is,

$$(\nabla \times H)_\theta = -\frac{1}{r}\frac{\partial(rH_\psi)}{\partial r}$$

Note also, that the resulting *E*-field is in terms of θ and is perpendicular to the *H*-field, as expected for electromagnetic plane waves.

$$rH_\psi = -i\,\frac{I\Delta l}{2\lambda}\,\sin\theta\left(1-\frac{1}{ikr}\right)e^{-i(\omega t-kr)}$$

$$= -i\,\frac{I\Delta l}{2\lambda}\,\sin\theta\,e^{-i\omega t}\left(e^{ikr}-\frac{e^{ikr}}{ikr}\right)$$

$$\frac{\partial(rH_\psi)}{\partial r} = -i\,\frac{I\Delta l}{2\lambda}\,\sin\theta\,e^{-i\omega t}\frac{\partial}{\partial r}\left(e^{ikr}-\frac{e^{ikr}}{ikr}\right)$$

We solve this using the quotient rule,

$$\left[\frac{u(r)}{v(r)}\right] = \frac{u'(r)v(r)-v'(r)u(r)}{v(r)^2} \qquad \begin{aligned} u(r) &= e^{ikr} & v(r) &= ikr \\ u'(r) &= ik\,e^{ikr} & v'(r) &= ik \end{aligned}$$

$$\frac{\partial}{\partial r}\left(e^{ikr} - \frac{e^{ikr}}{ikr}\right) = ik\,e^{ikr} - \left(\frac{ik\,e^{ikr}\cdot ikr - ik\cdot e^{ikr}}{(ikr)^2}\right)$$

$$= ik\,e^{ikr}\left(1 - \frac{1}{ikr} + \frac{1}{(ikr)^2}\right)$$

so,

$$\frac{\partial(rH_\psi)}{\partial r} = -i\,\frac{I\Delta l}{2\lambda}\,\sin\theta\,e^{-i\omega t}\,ik\,e^{ikr}\left(1 - \frac{1}{ikr} + \frac{1}{(ikr)^2}\right)$$

and,

$$-\frac{1}{r}\frac{\partial(rH_\psi)}{\partial r} = i^2 k\,\frac{I\Delta l}{2\lambda}\,\frac{\sin\theta}{r}\left(1 - \frac{1}{ikr} + \frac{1}{(ikr)^2}\right)\,e^{-i(\omega t - kr)}$$

we find,

$$k = \frac{\omega}{c}$$

$$E_\theta = -i\frac{1}{c\,\epsilon_0}\,\frac{I\Delta l}{2\lambda}\,\frac{\sin\theta}{r}\left(1 - \frac{1}{ikr} + \frac{1}{(ikr)^2}\right)\,e^{-i(\omega t - kr)}$$

So the E-field can also be expressed as,

$$c = \frac{1}{\sqrt{\mu_0\epsilon_0}}$$

$$E_\theta = -i\sqrt{\frac{\mu_0}{\epsilon_0}}\,\frac{I\Delta l}{2\lambda}\,\frac{\sin\theta}{r}\left(1 - \frac{1}{ikr} + \frac{1}{(ikr)^2}\right)\,e^{-i(\omega t - kr)}$$

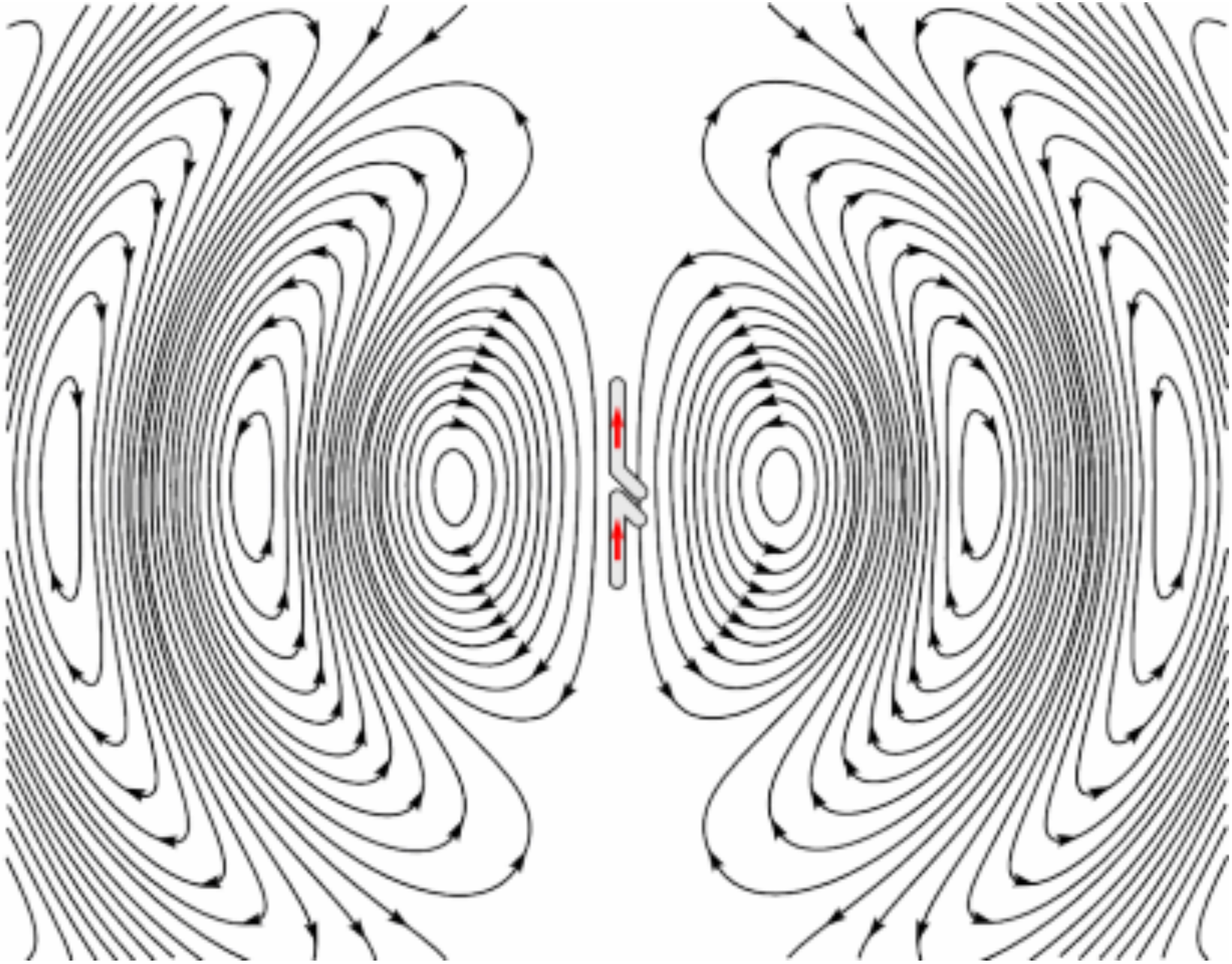

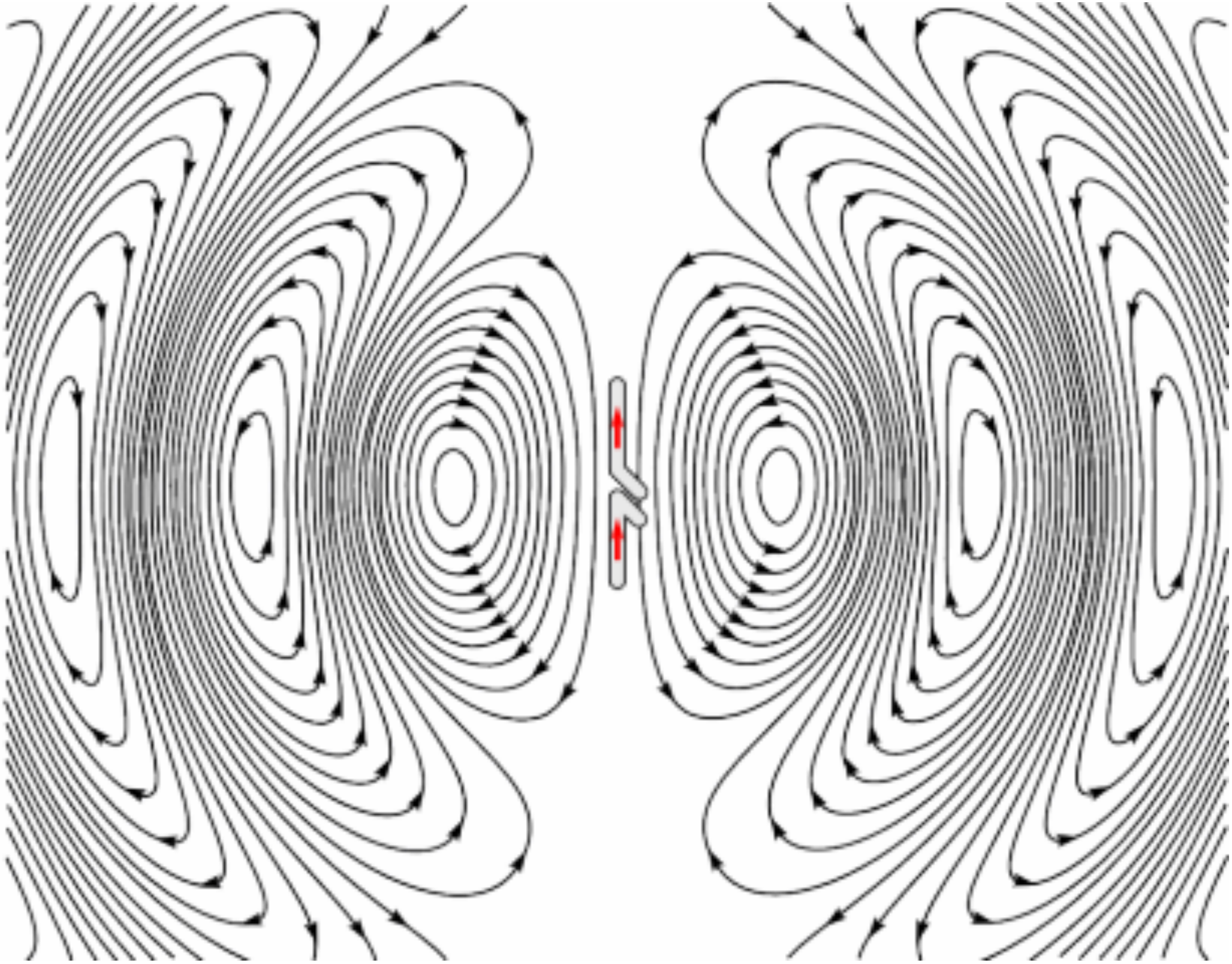

So, our electric and magnetic fields are,

$$H_\psi = -i\,\frac{I\Delta l}{2\lambda}\,\frac{\sin\theta}{r}\left(1-\frac{1}{ikr}\right)e^{-i(\omega t-kr)}$$

$$E_\theta = -i\sqrt{\frac{\mu_0}{\epsilon_0}}\,\frac{I\Delta l}{2\lambda}\,\frac{\sin\theta}{r}\left(1-\frac{1}{ikr}+\frac{1}{(ikr)^2}\right)\,e^{-i(\omega t-kr)}$$

There are several factors that depend on the power of the distance *r* from the antenna,

1. 1/r : The radiation field (dominates at large $r \gg \Delta l$).
2. $1/r^2$: The induction field
3. $1/r^3$: The static field (of the E-field).

To calculate the near-field properties, all factors must be evaluated, but in the far-field, where we measure the radiation from the antennas, the 1/r term dominates.

$$H_\psi = -i\frac{I\Delta l}{2\lambda}\,\frac{\sin\theta}{r}\,e^{-i(\omega t-kr)}$$

$$E_\theta = -i\sqrt{\frac{\mu_0}{\epsilon_0}}\,\frac{I\Delta l}{2\lambda}\,\frac{\sin\theta}{r}\,e^{-i(\omega t-kr)}$$

Note that,

$$\frac{|E|}{|H|} = \sqrt{\frac{\mu_0}{\epsilon_0}} = 1$$

in cgs units

4. We can now determine the directional power per unit area in the far-field by calculating the time-averaged Poynting vector.

$$\langle \vec{S} \rangle = \frac{1}{\mu_0} |\mathrm{Re}\ \vec{E} \times \vec{B}^*| = |\mathrm{Re}\ \vec{E} \times \vec{H}^*|$$

$$= \sqrt{\frac{\mu_0}{\epsilon_0}} \left(\frac{I \Delta l}{2\lambda} \right)^2 \frac{\sin^2 \theta}{r^2} \left(\frac{1}{2} \right)$$

where $\quad \langle \cos^2(\omega t) \rangle = \frac{1}{2}$

The radiation has doughnut shaped power pattern (angular distribution of radiated power) due to dependence on $\sin^2 \theta$.

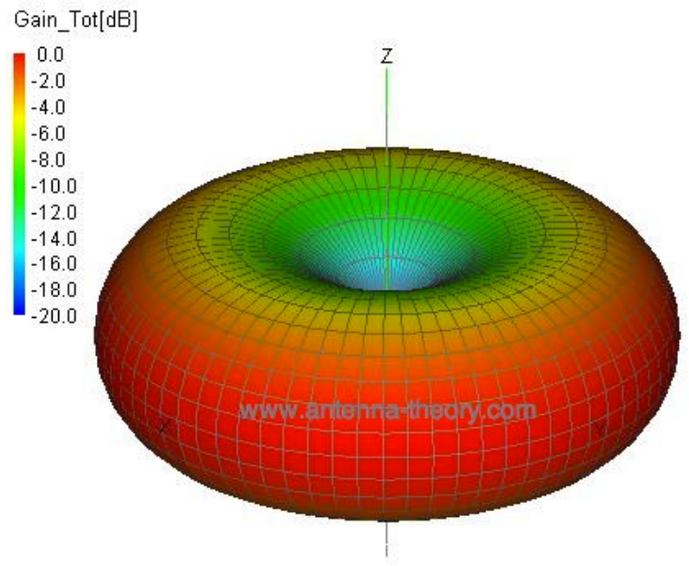

5. The time-average power radiated is then the integral of the Poynting vector over a whole sphere.

$$\langle P \rangle = \int_{\mathrm{sphere}} \langle S \rangle \, dA \quad = \sqrt{\frac{\mu_0}{\epsilon_0}} \left(\frac{I \Delta l}{2\lambda} \right)^2 \left(\frac{1}{2} \right) \int_{\phi=0}^{\phi=2\pi} \int_{\theta=0}^{\theta=\pi} \frac{\sin^2 \theta}{r^2} \, r^2 \sin\theta \, d\theta \, d\phi$$

$$\langle P \rangle = \frac{\pi}{3\, c\, \epsilon_0} \left(\frac{I \Delta l}{\lambda} \right)^2$$

2.2 Response of the LOFAR antenna:

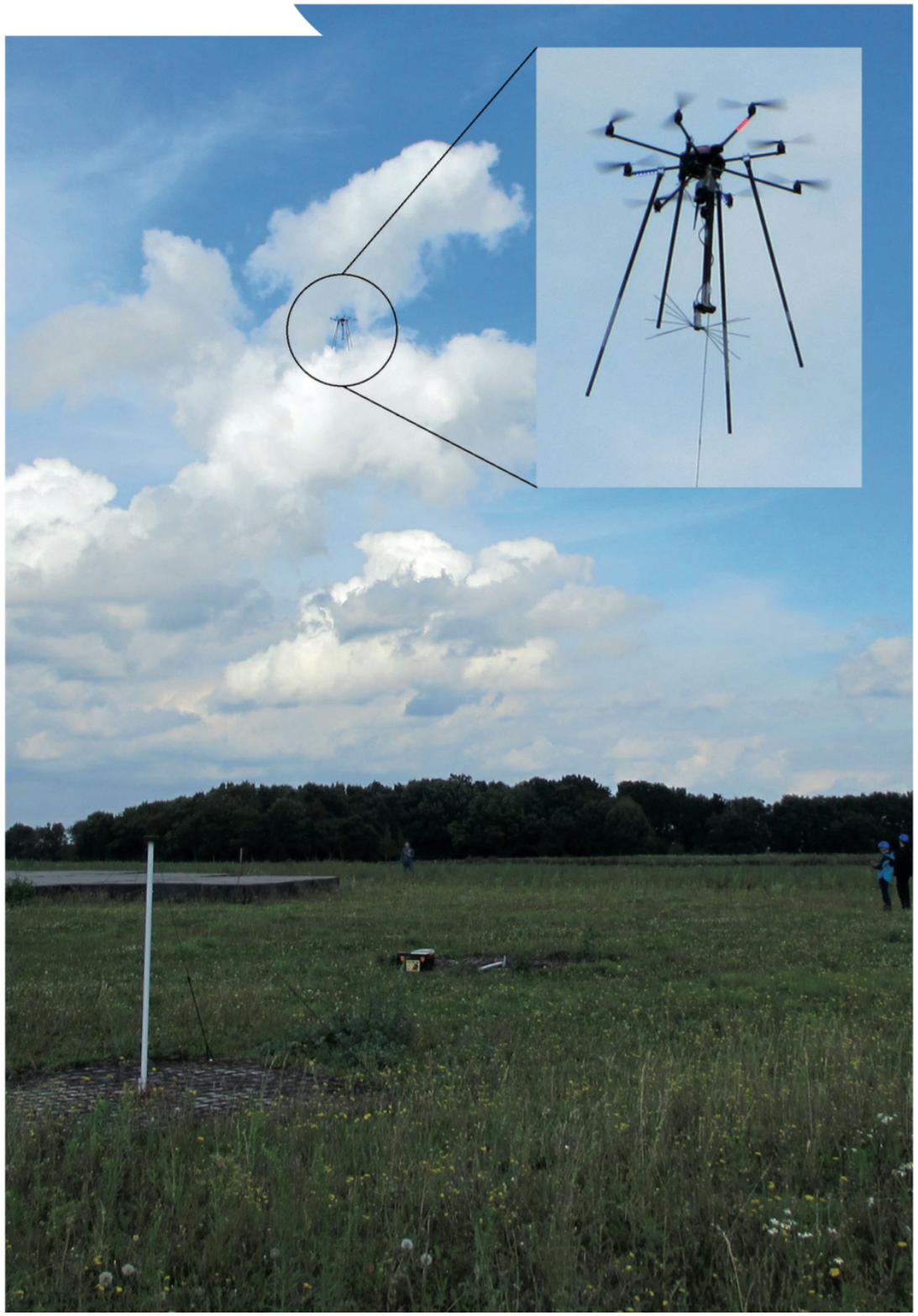

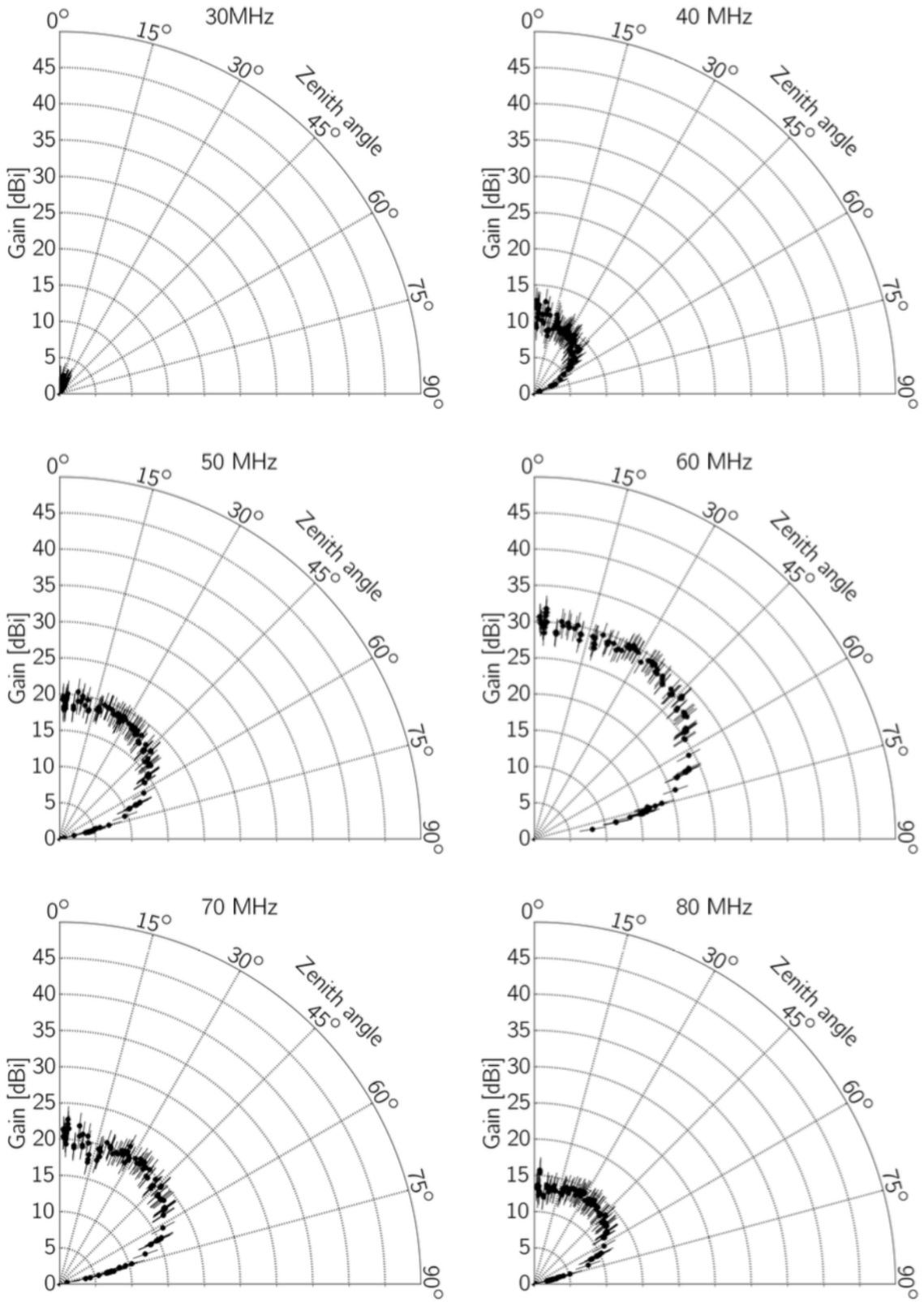

2.3 Power gain:

G(θ, ϕ) is the power transmitted per unit solid angle in direction *(θ, ϕ)* divided by the power transmitted per unit solid angle from an isotropic antenna with the same total power.

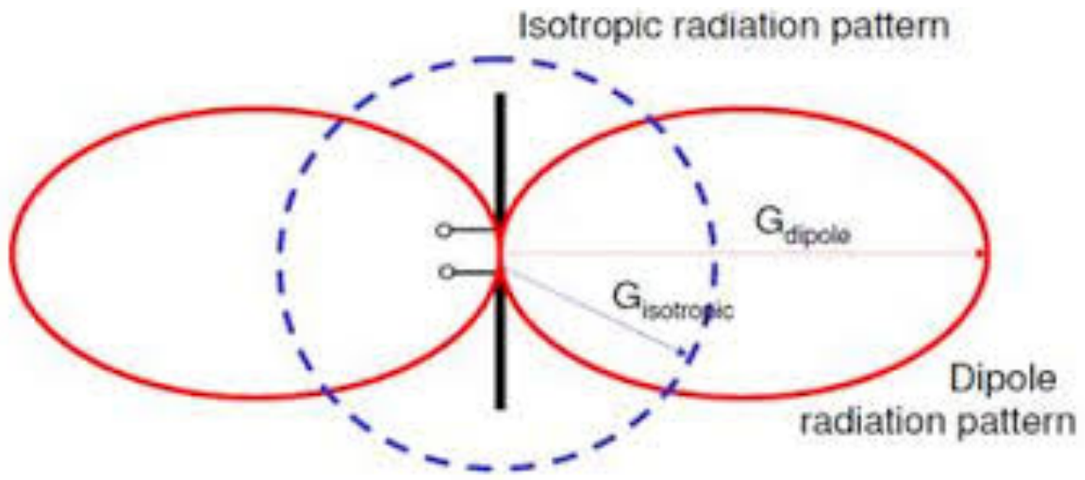

- The power or gain are often expressed in logarithmic units of decibels (dB):

$$G(\mathrm{dB}) \equiv 10 \times \log_{10}(\mathrm{G})$$

Worked example: What is the maximum and half power of a normalised power pattern in decibels?

2.3 Power gain:

G(θ, ϕ) is the power transmitted per unit solid angle in direction *(θ, ϕ)* divided by the power transmitted per unit solid angle from an isotropic antenna with the same total power.

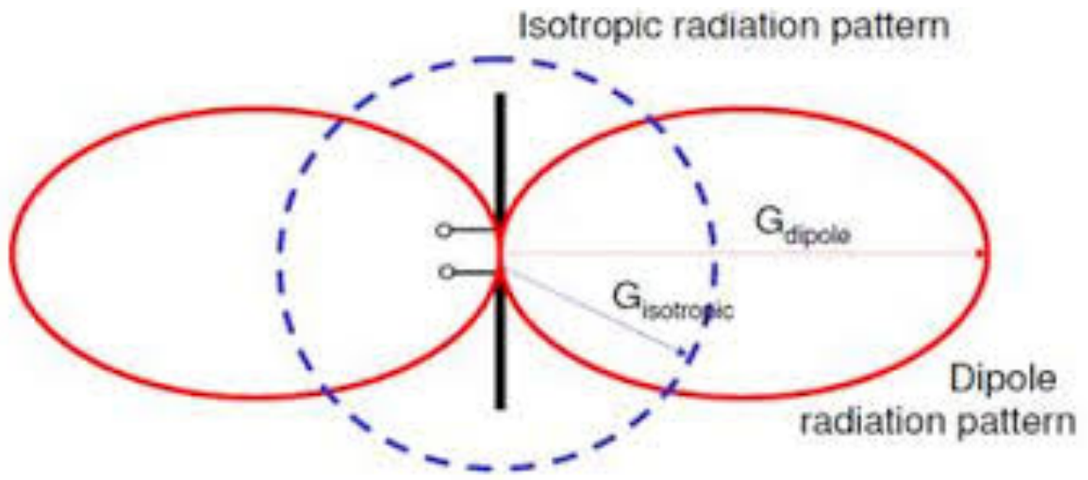

- The power or gain are often expressed in logarithmic units of decibels (dB):

$$G(\mathrm{dB}) \equiv 10 \times \log_{10}(\mathrm{G})$$

Worked example: What is the maximum and half power of a normalised power pattern in decibels?

Maximum power of a normalised power pattern is $P_n = 1$

$$P_n(1) = 10 \times \log_{10}(1) = 0 \text{ dB}$$

Half power of a normalised power pattern is $P_n = 0.5$

$$P_n(0.5) = 10 \times \log_{10}(0.5) = -3 \text{ dB}$$

For a lossless isotropic antenna, conservation of energy requires the directive gain averaged over all directions be,

$$\langle G \rangle \equiv \frac{\int_{\text{sphere}} G d\Omega}{\int_{\text{sphere}} d\Omega} = 1$$

Therefore, for an isotropic lossless antenna,

$$\int_{\text{sphere}} G d\Omega = \int_{\text{sphere}} d\Omega = 4\pi \qquad \text{and} \qquad G = 1$$

- Lossless antennas may radiate with different directional patterns, but they cannot alter the total amount of power radiated —> the gain of a lossless antenna depends only on the angular distribution of radiation from that antenna.

Key Concept: Higher the gain, the narrower the radiation pattern (directivity).

$$\Delta\Omega \approx \frac{4\pi}{G_{\text{max}}}$$

2.4 Effective collecting area

- The receiving counterpart of the transmitting gain is the effective collecting area, defined as the product of the geometric area and the incident spectral power per unit area (S_ν, the flux-density),

Effective area (m^2)

$$A_e \equiv \frac{P_\nu}{S_{(\mathrm{matched})}}$$

Spectral power (W Hz^{-1})

Flux-density (W m^{-2} Hz^{-1})

We can relate the effective area with the geometric area via the aperture efficiency,

$$A_\mathrm{e} = \eta_\mathrm{A} A_\mathrm{g}$$

Any antenna with a single output measures only one polarisation. Electric fields perpendicular to the antenna wires does not produce currents in the antenna. A pair of crossed dipoles are need to collect the power from both polarisations.

- For an unpolarised source (e.g. like a black body),

$$S_{(\mathrm{matched})} = \frac{S}{2}$$

- The total spectral power from all directions collected by the antenna is,

$$P_\nu = A_e S_{(\text{matched})} = A_e \frac{S}{2} = \int_{4\pi} A_e(\theta,\phi)\frac{B_\nu}{2} d\Omega = kT$$

(must equal the Nyqvist spectral power). From the R-J equation,

$$B_\nu = \frac{2kT}{\lambda^2} \qquad P_\nu = \frac{2kT}{2\lambda^2}\int_{4\pi} A_e(\theta,\phi)d\Omega = kT$$

$$\int_{4\pi} A_e(\theta,\phi)d\Omega = \lambda^2$$

- The average collecting area is defined as

$$\langle A_e \rangle = \frac{\int_{4\pi} A_e(\theta,\phi)d\Omega}{\int_{4\pi} d\Omega}$$

The effective collecting area is independent of the antenna environment, so this relation is valid for any type of radiation (not just black body radiation).

Key concept: Any antenna has the same average collecting area $\langle A_e \rangle$ that depends only on the wavelength of the radiation. $\langle A_e \rangle = \frac{\lambda^2}{4\pi}$

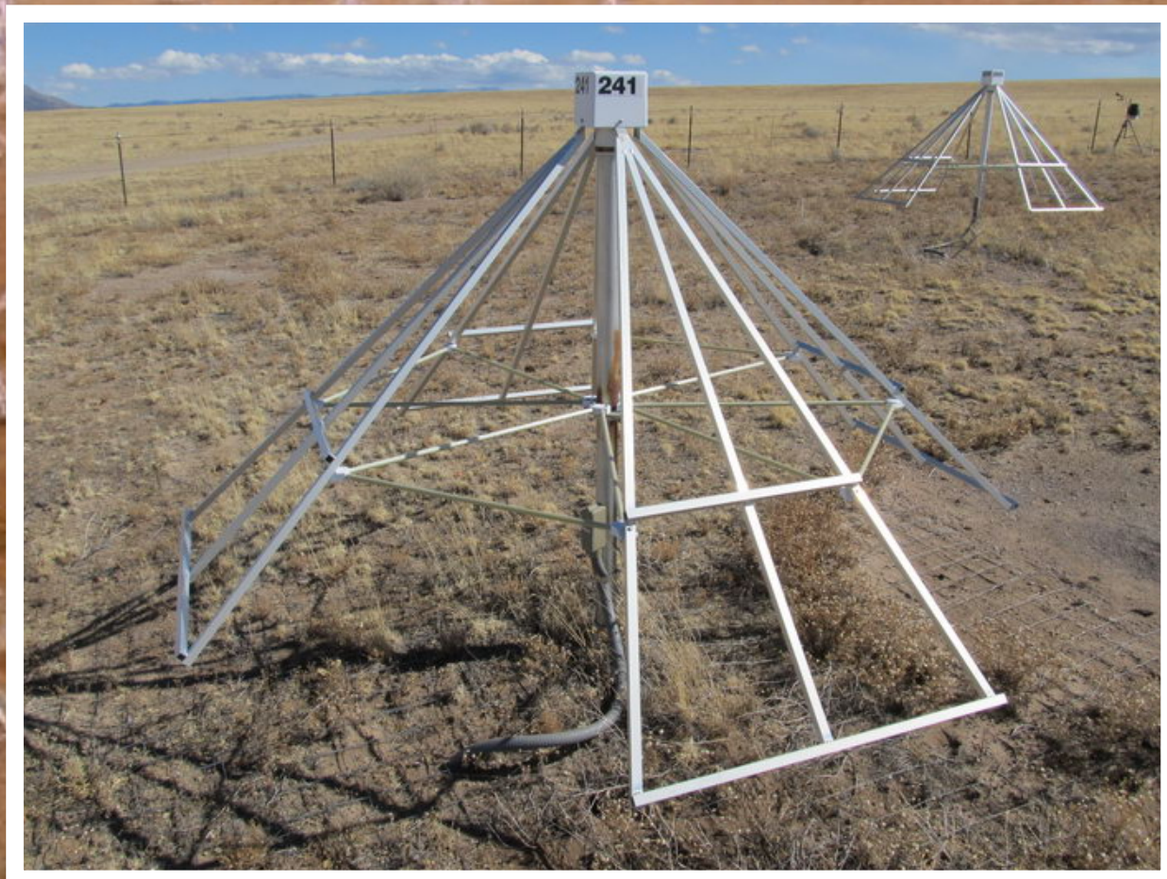
241

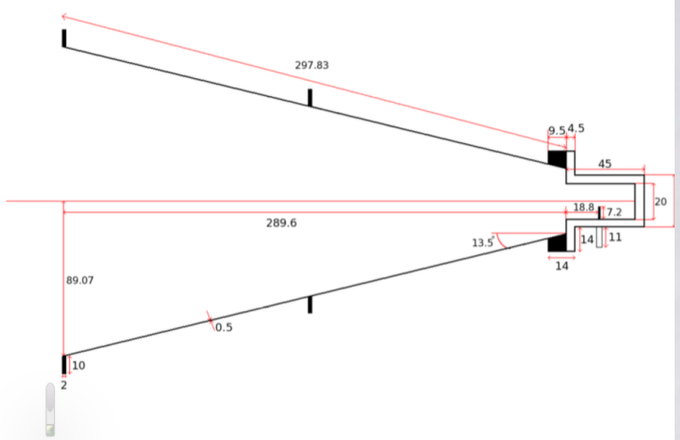
297.83
9.5
4.5
45
20
18.8
7.2
289.6
13.5
14
11
14
89.07
0.5
10
2

- Beam solid angle: The beam area Ω_A is the solid angle through which all of the power radiated by the antenna would stream if $P(\theta, \phi)$ maintained its maximum value over Ω_A and zero everywhere else.

Normalised power pattern

Beam solid angle (sr)

$$\Omega_{\mathrm{A}} \equiv \int_{4\pi} P_{\mathrm{n}}(\theta, \phi) d\Omega$$

sky area ($r^2 \sin\theta \, d\theta d\phi$)

The power (and temperature) received is also a function of the power pattern of the antenna. Therefore, the true antenna temperature is,

$$T_{\mathrm{A}} = \frac{A_{\mathrm{e}}}{2k} \int \int I_{\nu}(\theta, \phi) P_{\mathrm{n}}(\theta, \phi) d\Omega$$

where $P_n(\theta, \phi)$ is the power pattern normalised to unity maximum,

$$P_{\mathrm{n}} = \frac{G(\theta, \phi)}{G_{\mathrm{max}}}$$

- Main beam solid angle: The area containing the principle response out to the first zero.

- Side-lobes: Areas outside the principle response that are non-zero.

$$\Omega_{\mathrm{MB}} \equiv \int_{\mathrm{MB}} P_{\mathrm{n}}(\theta,\phi)\,d\Omega$$

Main beam solid angle (sr)

- Main beam efficiency: The fraction of the total beam solid angle inside the main beam

Main beam efficiency

$$\eta_{\mathrm{B}} \equiv \frac{\Omega_{\mathrm{MB}}}{\Omega_{\mathrm{A}}}$$

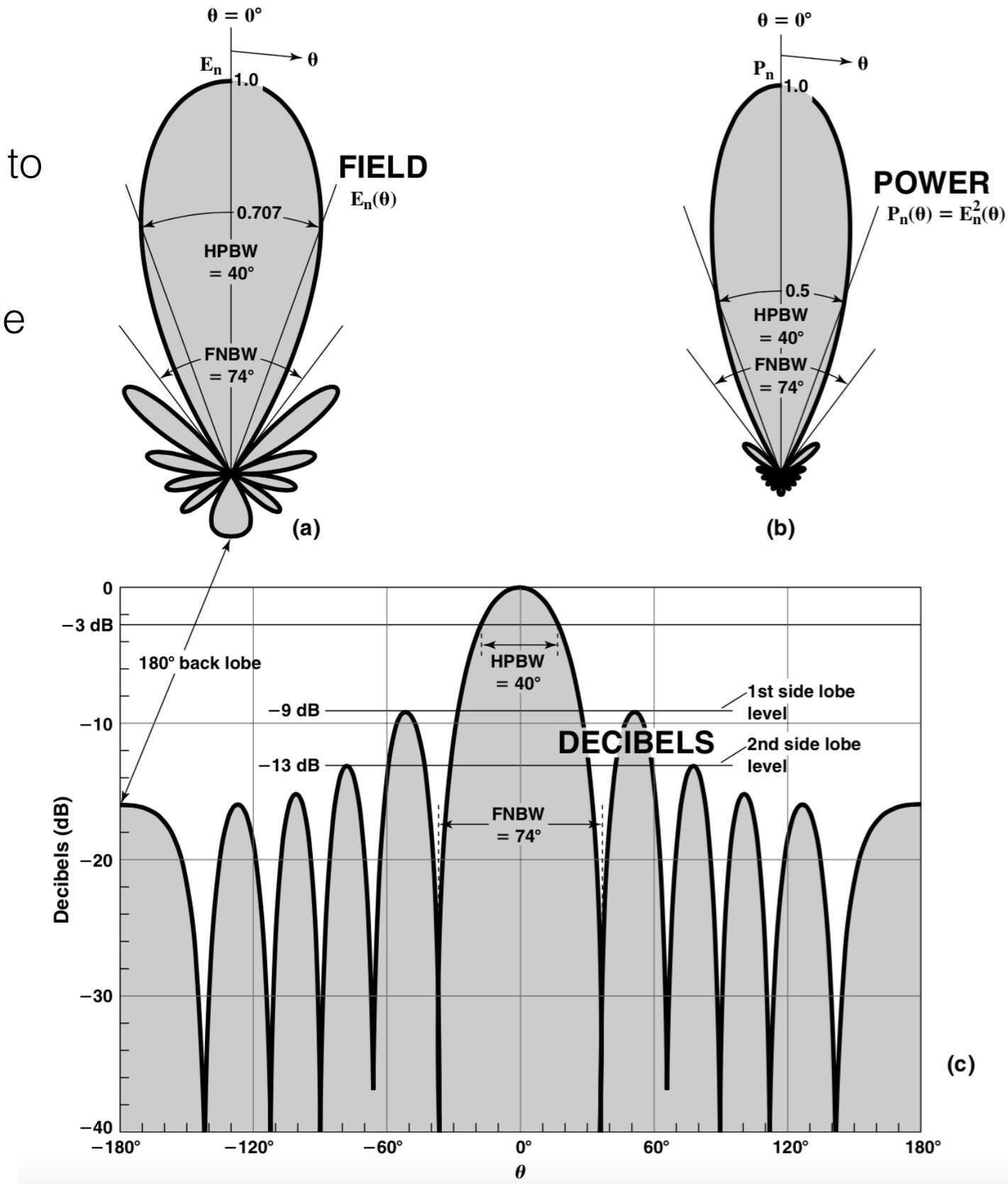

3.1 Interferometers

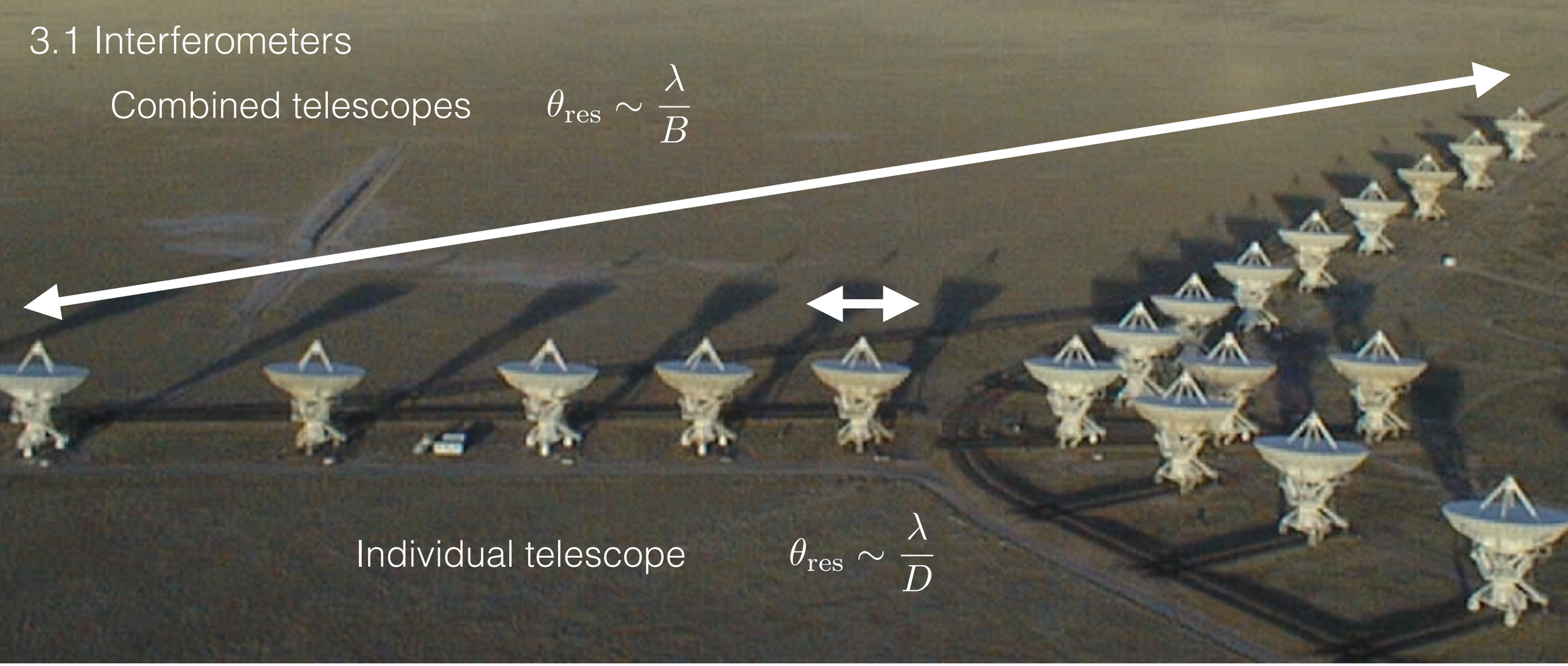

- We can overcome this problem by correlating the signals from different telescopes to effectively increase *D* to an arbitrarily large value by increasing the distance between the telescopes, called the baseline length *B*. Now, $\theta \sim \lambda / B$.
    1. High angular resolution (down to < 1 mas; best in astronomy), e.g. VLBI.
    2. Better sensitivity (Area = $N\pi D^2/4$, *N* is number of telescopes), e.g. LOFAR, JVLA, ALMA.
    3. Large field-of-view (10s deg^2) in the case of phased array feeds, e.g. WSRT-Aperitif.

3.2 Young's double slit experiment

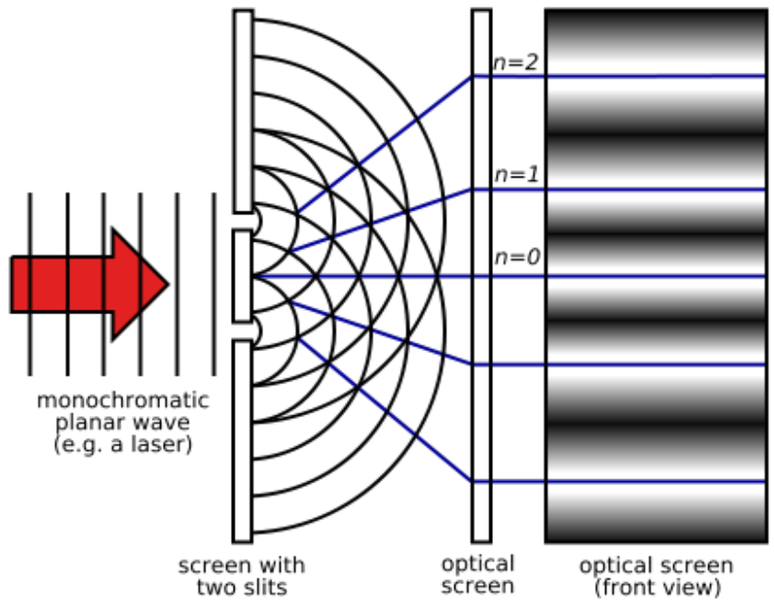

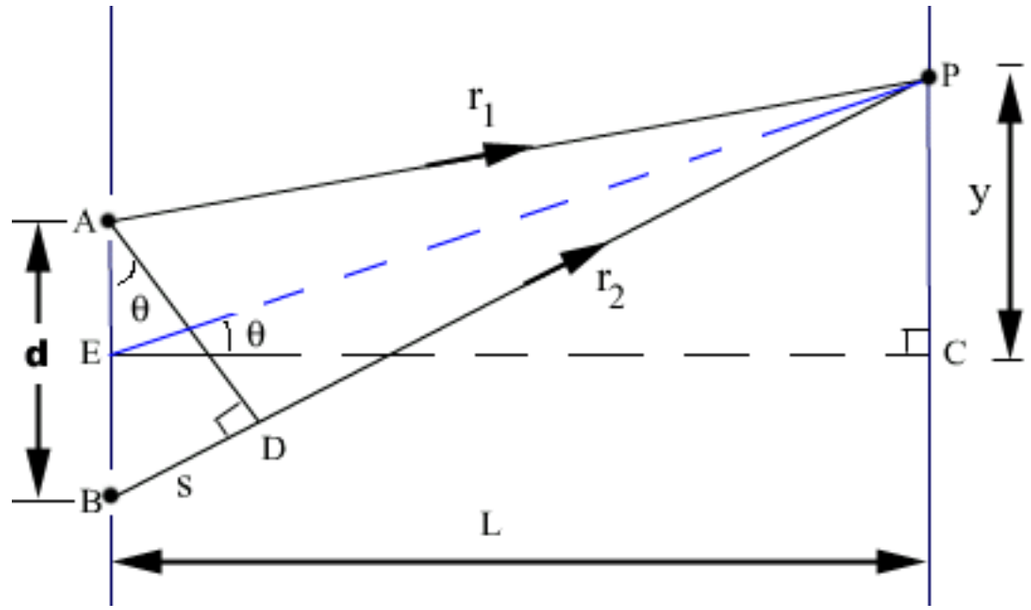

Constructive interference fringes occur when the path difference is an integer number wavelengths, i.e.

$$d \sin\theta = n\lambda \quad \text{and for destructive interference,} \quad d \sin\theta = (n + 1/2)\lambda$$

when $y \ll L$, we can approximate $\sin\theta = y / L$ and the positions of the maxima and minina are,

$$y_c = \frac{n\lambda L}{d} \qquad \text{and} \qquad y_d = \frac{(n + 1/2)\lambda L}{d}$$

and the spacing between successive fringes is,

$$\Delta y = \frac{\lambda L}{d} \qquad \text{or, expressed as an angular size,} \qquad \theta \sim \frac{\lambda}{d}$$

3.3 A simple two-element interferometer

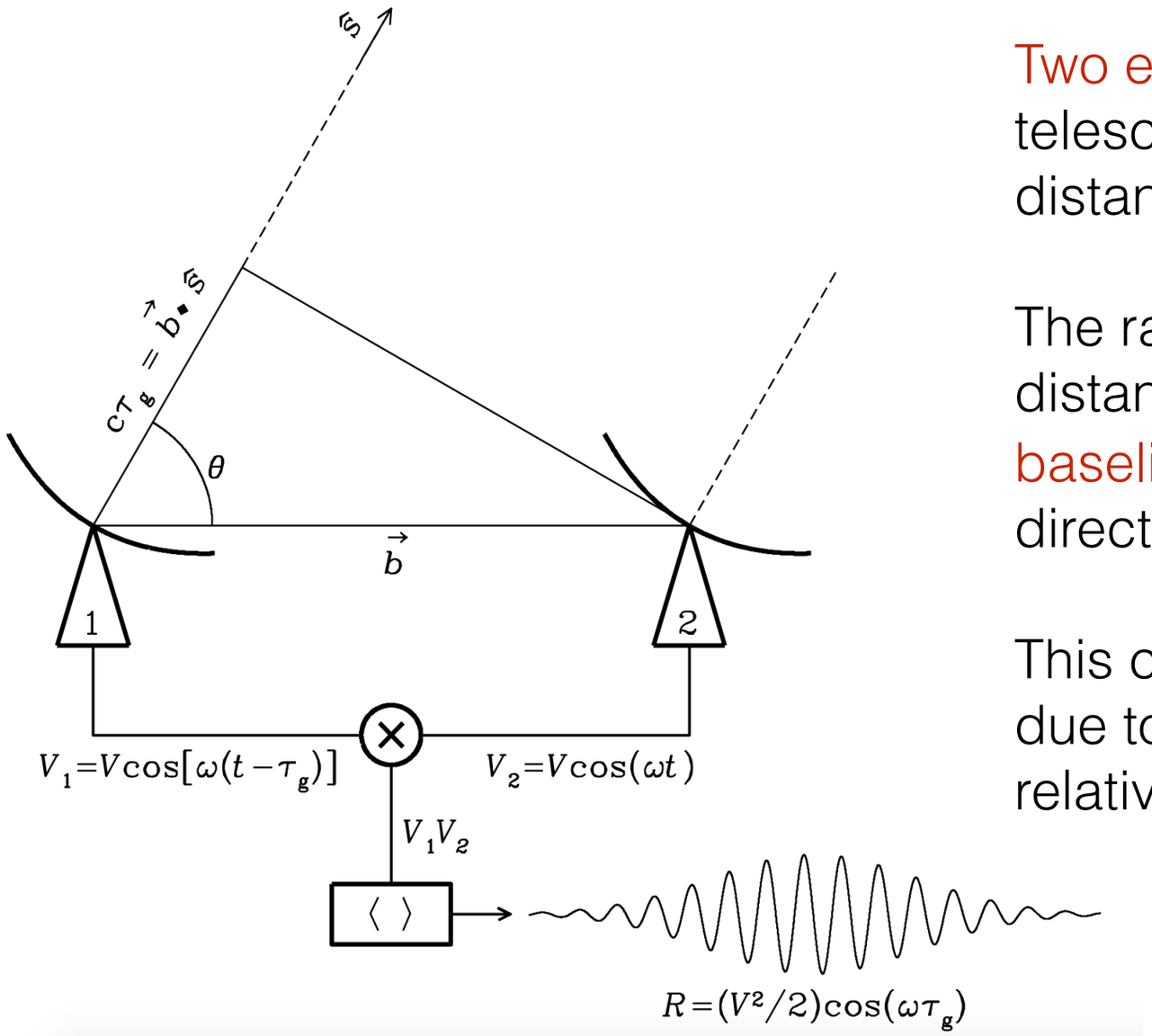

Two element interferometer: Two identical telescopes observe the electric field of some distant source (c.f. Young's double slit).

The radiation to antenna 1 travels an extra distance $\mathbf{b} \cdot \hat{\mathbf{s}} = b \cos\theta$, where $\mathbf{b}$ is the vector baseline length and $\hat{\mathbf{s}}$ a unit vector in the direction of the source.

This can be expressed as a geometric delay due to the projected position of the source, relative to the baseline of the antennas.

$$\tau_g = \vec{b} \cdot \hat{s}/c$$

For a quasi-monochromatic interferometer (responds to a narrow frequency range $\nu = 2\pi / \lambda$), the output voltages over time t from the two antennas are,

$$V_1 = V\cos[\omega(t-\tau_g)] \quad \text{and} \quad V_2 = V\cos(\omega t)$$

The correlator multiples the voltages from the two antennas together to give,

$$V_1 V_2 = V^2 \cos[\omega(t-\tau_g)]\cos(\omega t) = \left(\frac{V^2}{2}\right)[\cos[2\omega t - \omega\tau_g] + \cos(\omega\tau_g)]$$

and then a time average [$\Delta t \gg (2\omega)^{-1}$] to remove the high frequency component to give,

$$R = \langle V_1 V_2 \rangle = \left(\frac{V^2}{2}\right)\cos(\omega\tau_g)$$

Uncorrelated noise from gain variations within the receivers, the atmosphere and radio frequency interference does not correlate (advantage over single dish measurements).

The output voltage *R* varies sinusoidally with the change of the source direction in the interferometer frame, i.e. the delay changes. These sinusoids are called fringes, and we can define the fringe phase as,

$$\phi = \omega\tau_g = \frac{\omega}{c} b\cos\theta \qquad \text{and} \qquad \frac{d\phi}{d\theta} = \frac{\omega}{c} b\sin\theta = 2\pi\left(\frac{b\sin\theta}{\lambda}\right)$$

The fringe period ($\Delta\phi = 2\pi$) corresponds to an angular change of $\Delta\theta = \lambda / (b \sin\theta)$, and so, for large *b,* interferometers can measure very accurate positions of sources (typically $\sigma_\theta \sim 10^{-3}$ arcsec).

As the source(s) moves across the sky, the response of the interferometer changes because the geometric delay changes. The maximum in the fringe pattern occurs when $\tau_g c$ is an integral number of wavelengths (similar to the Young's double slit).

This effect of combining antennas changes the response of our instrument to the sky.

a. The power pattern of a filled aperture of diameter *D* with a constant illumination pattern. The FWHM of the main beam is ~ λ / *D.*

b. The power pattern of a two-element interferometer with 2 antennas of diameter *d* and separation *D.* The side-lobe level is constant and the power is centred on 0. The FWHM of the fringes is ~ λ / *D.*

c. The power pattern of a two-element interferometer with 2 antennas of diameter *d* and separation 2*D.* The FWHM of the fringes is now ~ λ / 2*D.*

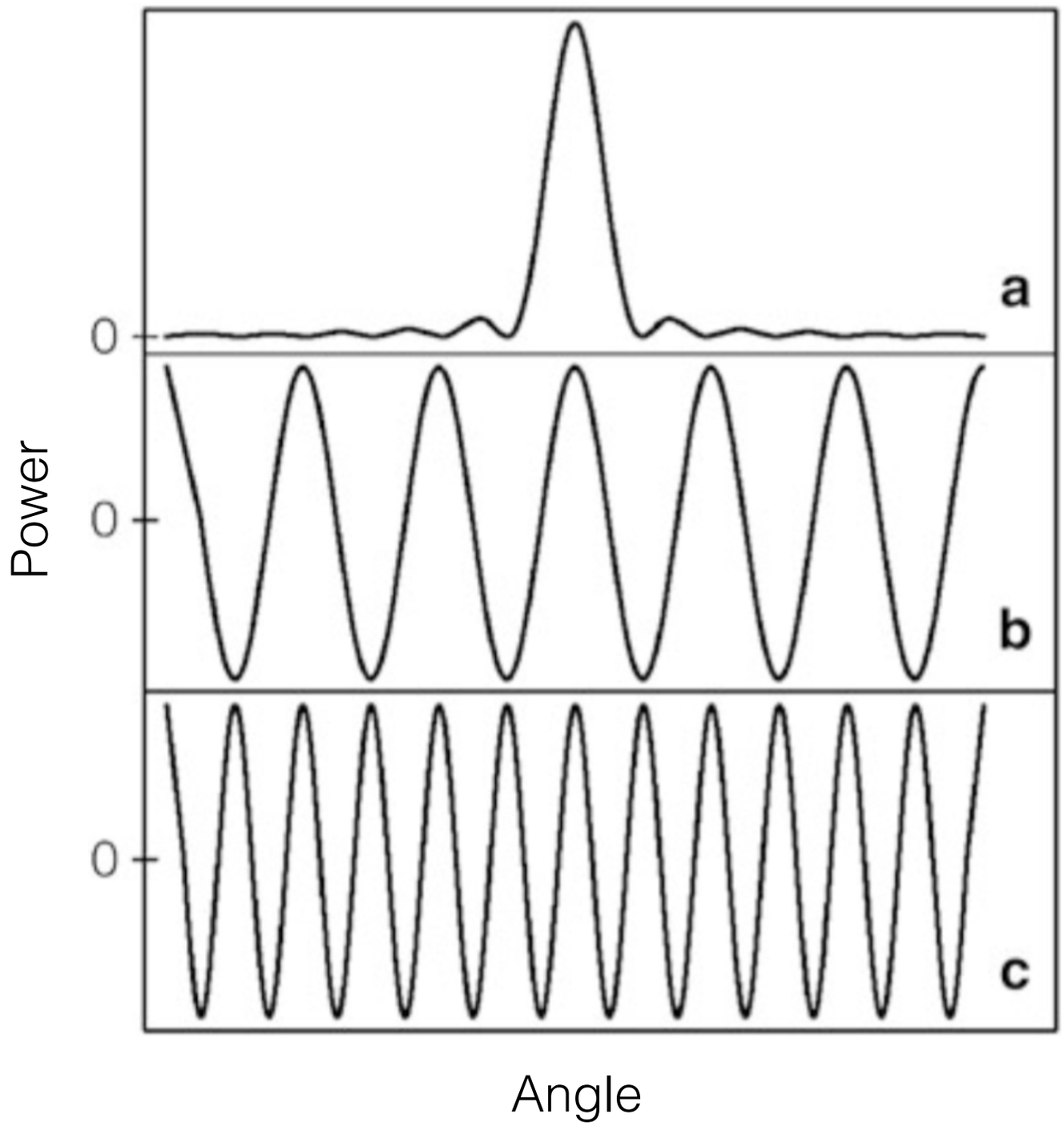

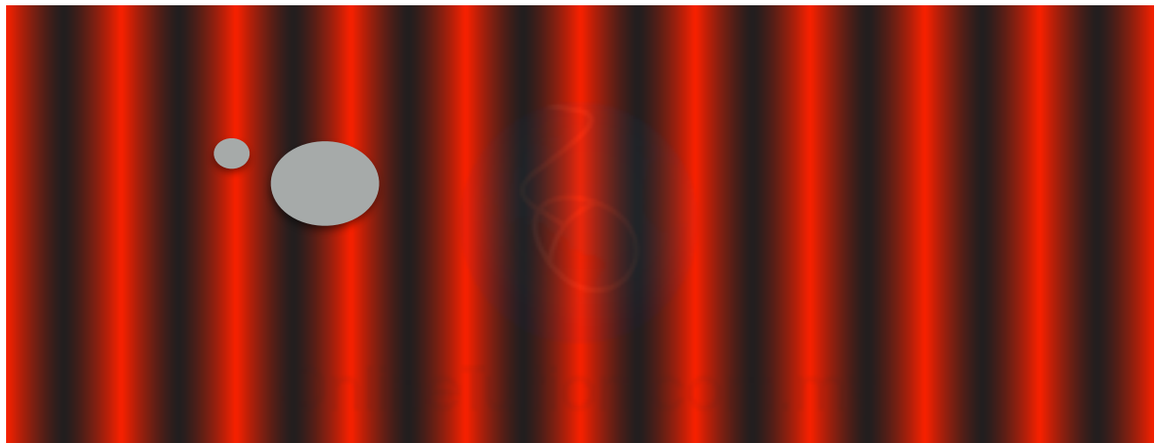

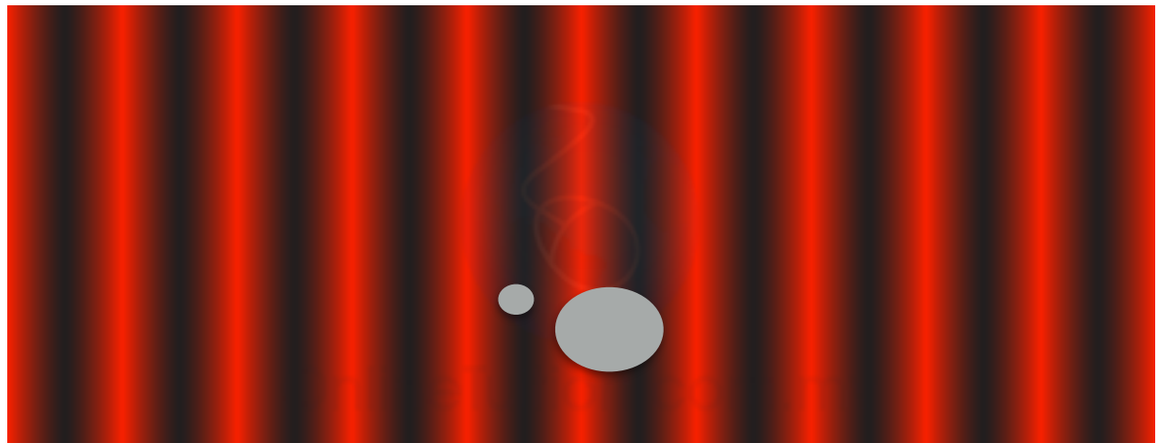

For sources much larger than adjacent positive and negative fringes, the source cancels itself out and the interferometer response does not vary.

Each set of antennas correspond to a finite set of angular frequencies centred on (b sin θ / λ), small b is needed for extended objects and large b is needed for compact objects.

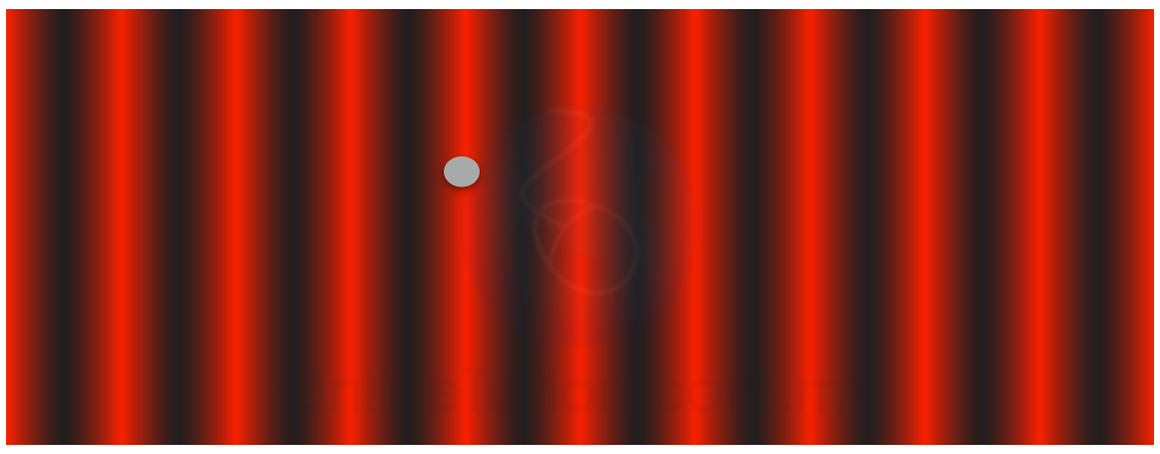

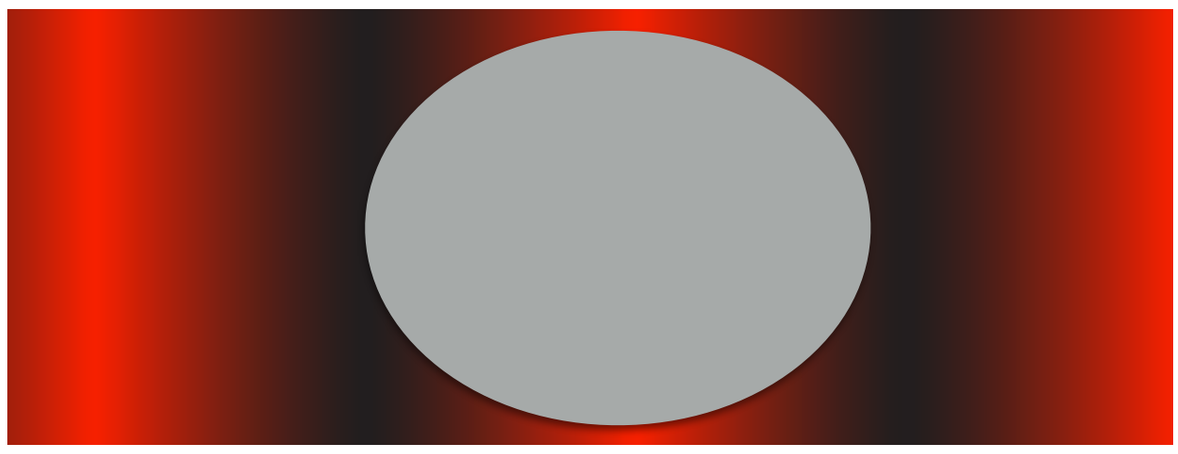

3.4 Extended sources

A spatially incoherent extended source with sky brightness $I_\nu(\hat{s})$ near frequency $\nu = \omega / 2\pi$ can be considered as the sum of independent point sources. The response of an interferometer is then,

$$R_c = \int I_\nu(\hat{s}) \cos(2\pi\nu\vec{b} \cdot \hat{s}/c) d\Omega = \int I_\nu(\hat{s}) \cos(2\pi\vec{b} \cdot \hat{s}/\lambda) d\Omega$$

Note that, the output from the correlator is a complex quantity and so far we have only considered the (real) cosine part of the signal. The (imaginary) sine component is found by inserting a 90^0 phase delay ($t - \tau_g - \pi/2$).

$$R_s = \int I_\nu(\hat{s}) \sin(2\pi\vec{b} \cdot \hat{s}/\lambda) d\Omega$$

It is convenient to express this in terms of complex exponentials,

$$e^{i\phi} = \cos\phi + i \sin\phi$$

Allowing us to define the complex visibility $V = R_c - iR_s$ as,

$$V = Ae^{-i\phi}$$

where the amplitude is, $A = (R_c^2 + R_s^2)^{1/2}$ and the phase is, $\phi = \tan^{-1}(R_s/R_c)$

So, we can write the response of a two element interferometer to an extended source with brightness distribution $I_\nu(\hat{s})$ as,

$$V_\nu = \int I_\nu(\hat{s}) \exp(-i2\pi\vec{b} \cdot \hat{s}/\lambda) d\Omega$$

3.5 General response of an interferometer

First, we define our co-ordinate systems.

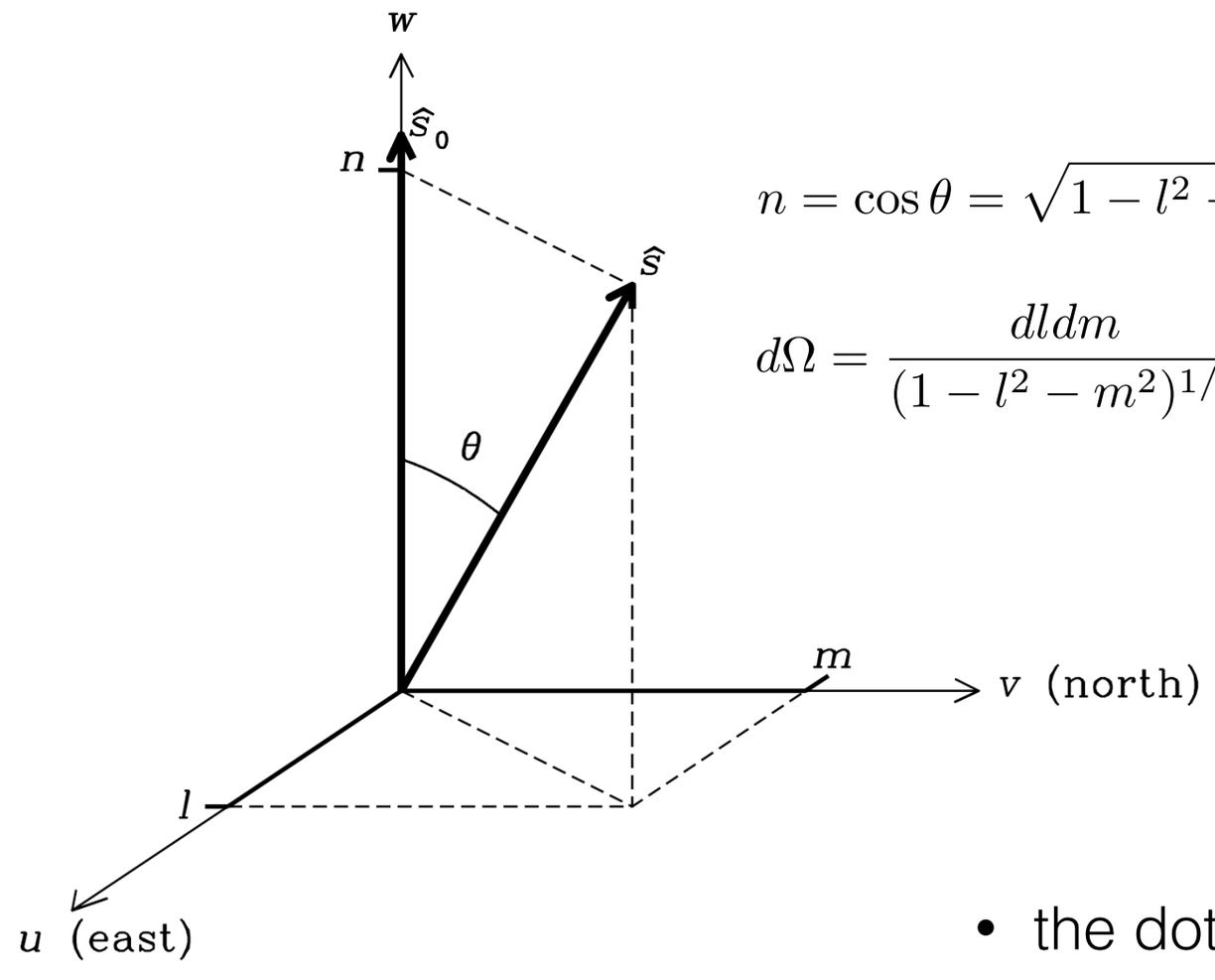

$$n = \cos\theta = \sqrt{1 - l^2 - m^2}$$

$$d\Omega = \frac{dldm}{(1 - l^2 - m^2)^{1/2}}$$

- baseline $\frac{\vec{b}}{\lambda} = (u, v, w)$ (North-South, East-West, Up-Down)
- source $\hat{s} = (l, m, \sqrt{1 - l^2 - m^2})$ (North-South, East-West, Up-Down)
- the dot product $\frac{\vec{b}}{\lambda} \cdot \hat{s} = ul + vm + w\sqrt{1 - l^2 - m^2}$

We can then describe the response of an interferometer to any position in the sky as,

$$V_\nu(u,v,w) = \int\int \frac{I_\nu(l,m)}{(1-l^2-m^2)^{1/2}} \exp[-i2\pi(ul+vm+wn)]dldm$$

Key Concept: The response of an interferometer is the (inverse) Fourier transform of the (apparent) sky brightness distribution.

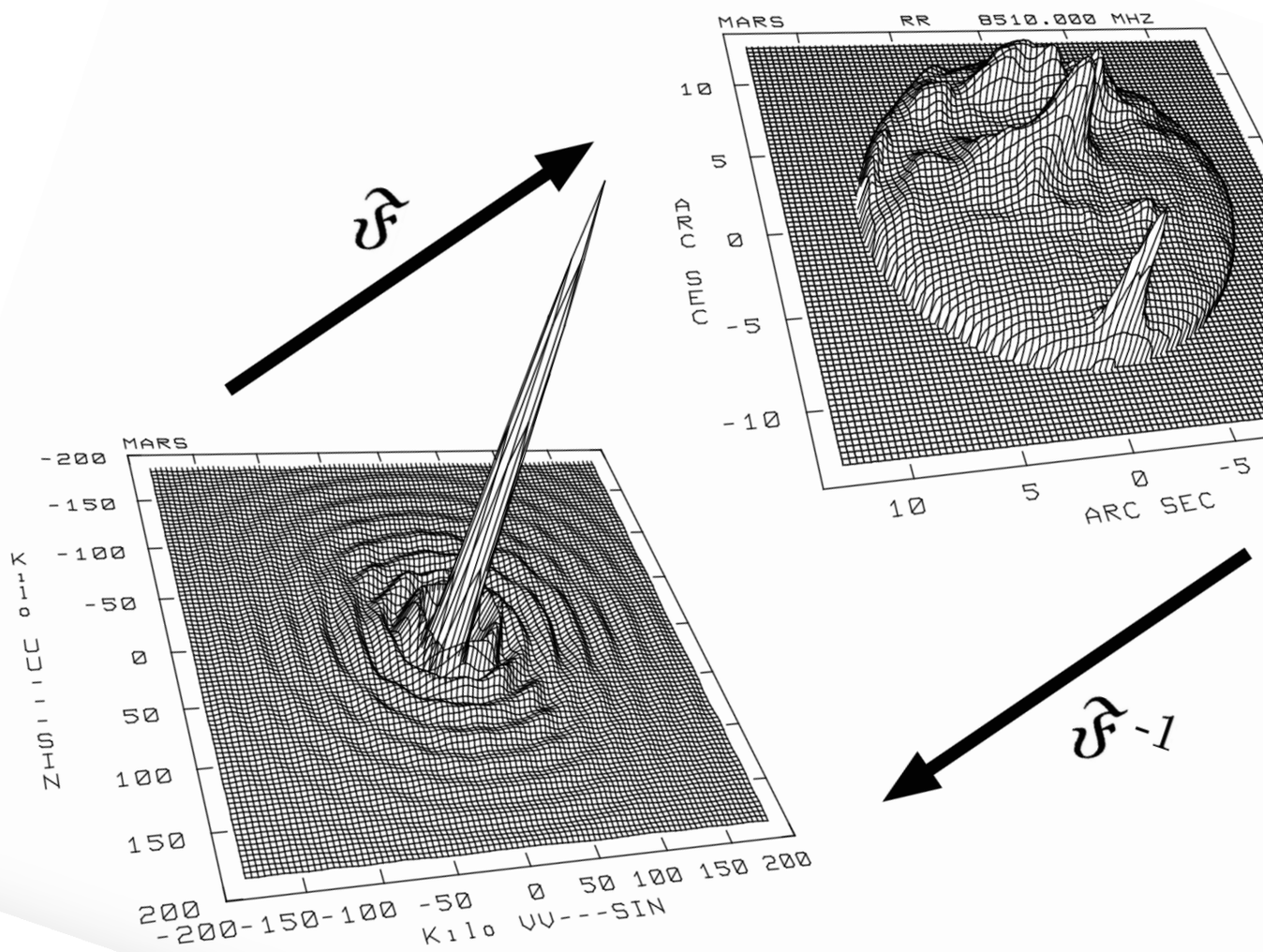

- Worked example: Here is the surface brightness distribution of Mars, as seen at 3.6 cm.
- An interferometer will see the Fourier transform of this surface brightness distribution.

- Incomplete measurement of the Fourier plane results in significant structure in the point spread function response of the interferometer.

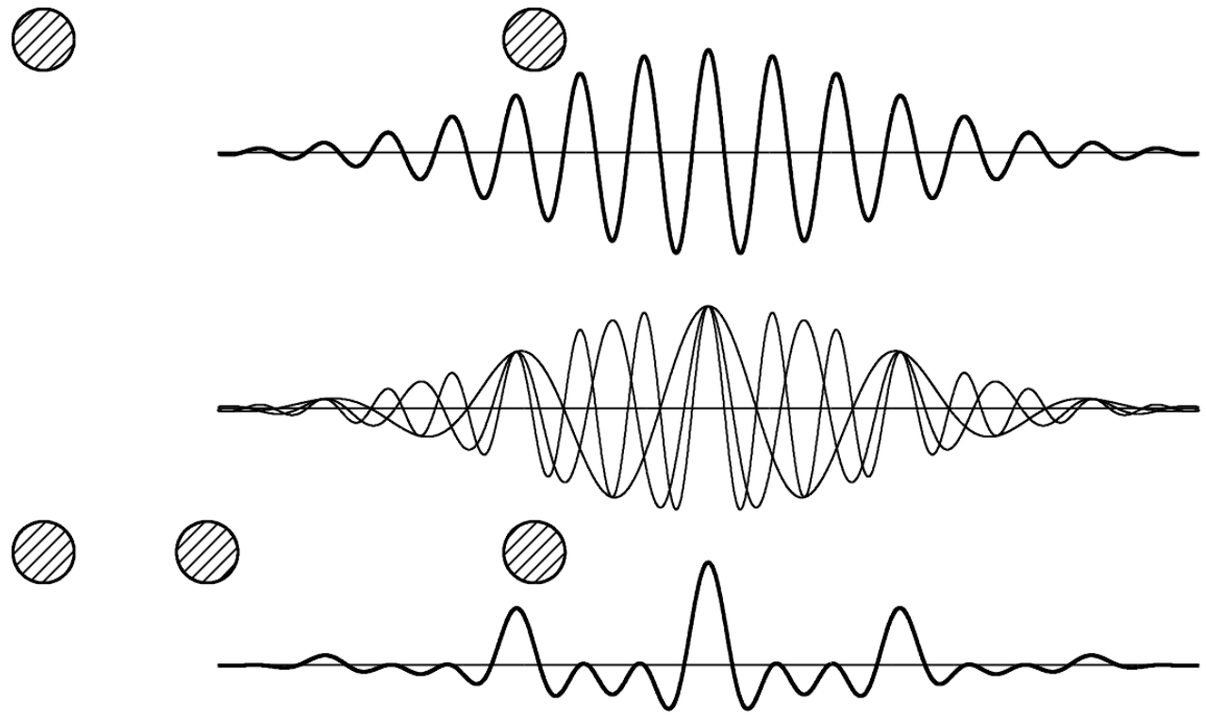

- Two antennas
- Three antennas

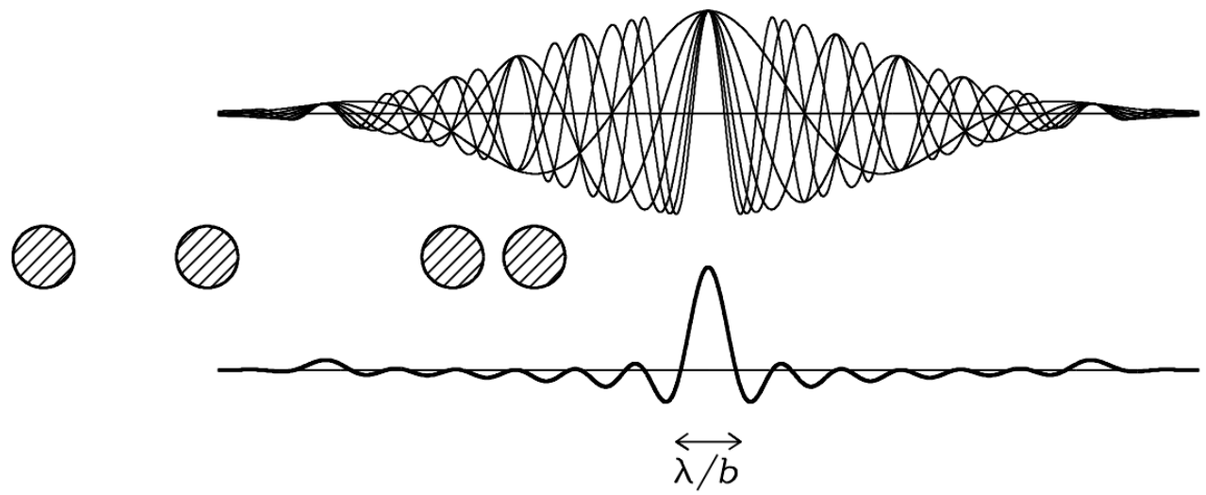

- Four antennas

- Negative bowl around the centre is due to the lack of information at short spacings (*b* cannot be < *D*, the antenna diameter).

Worked example: The combined 24 tiles of a LOFAR High Band Antenna station (120-250 MHz) arranged in a regular grid.

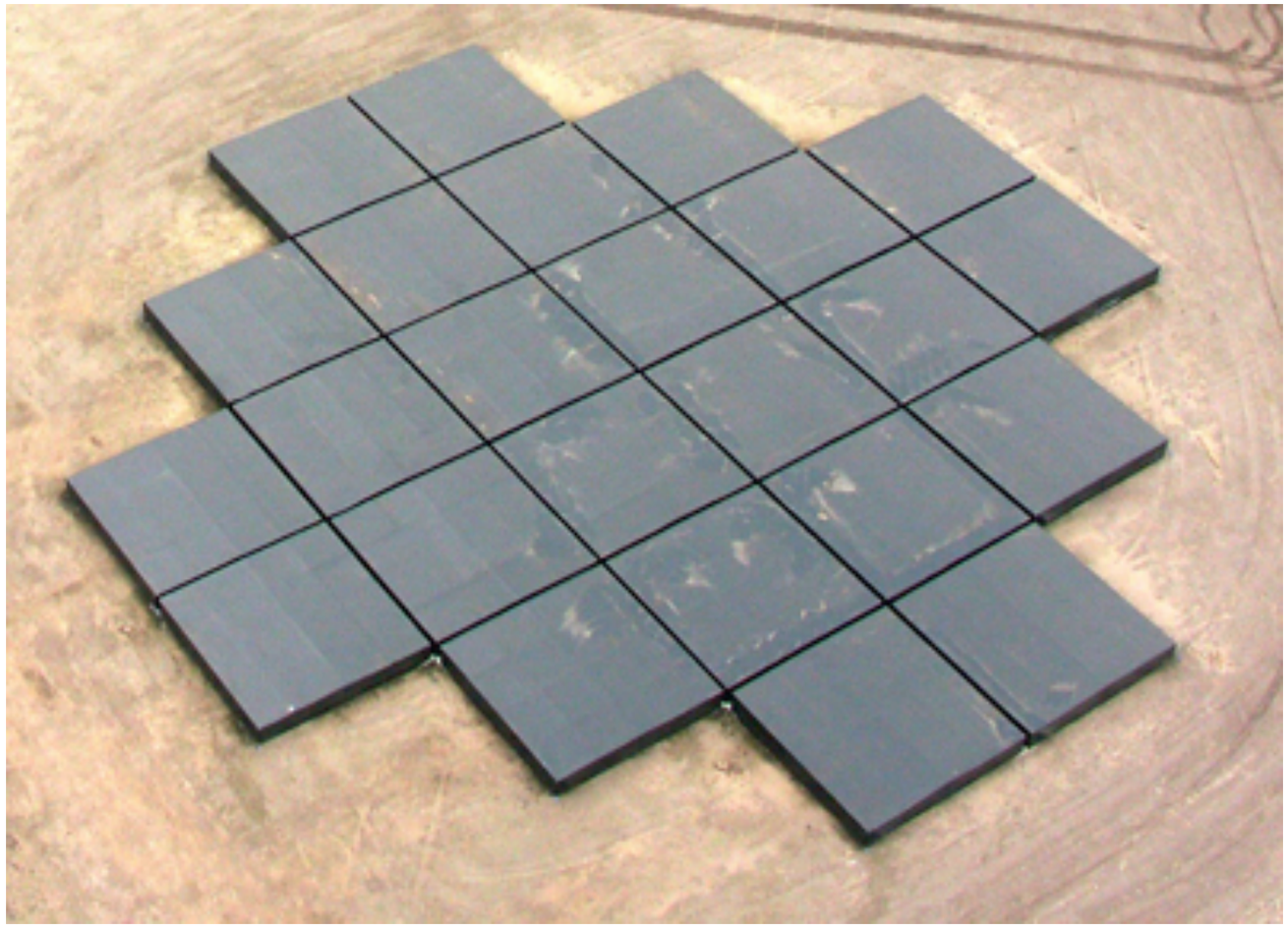

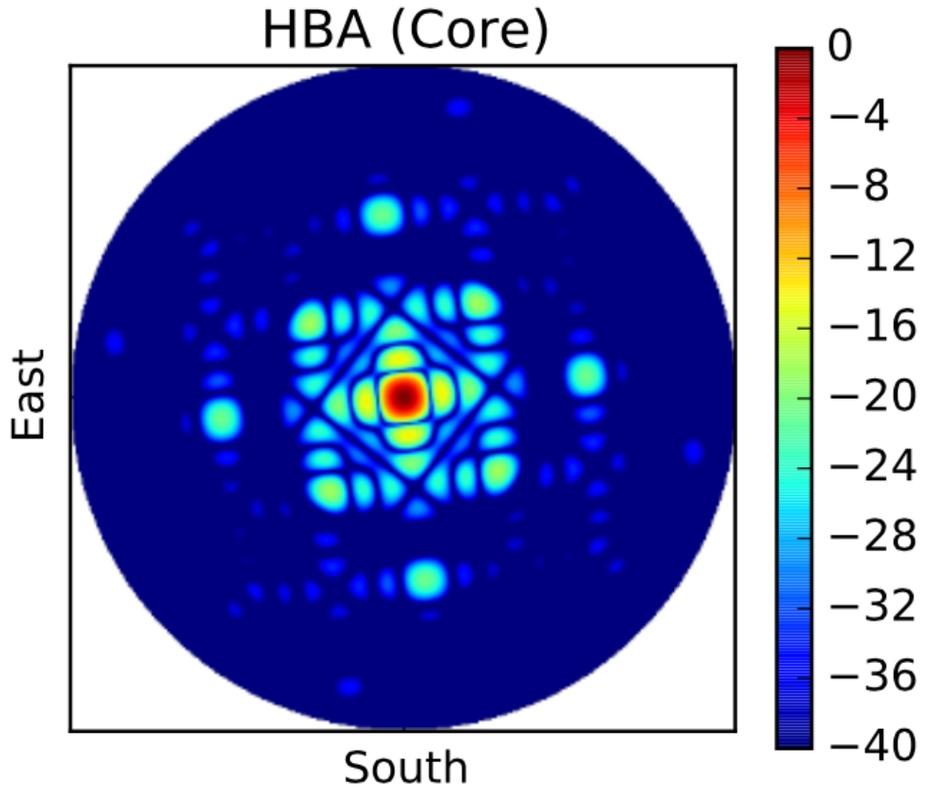

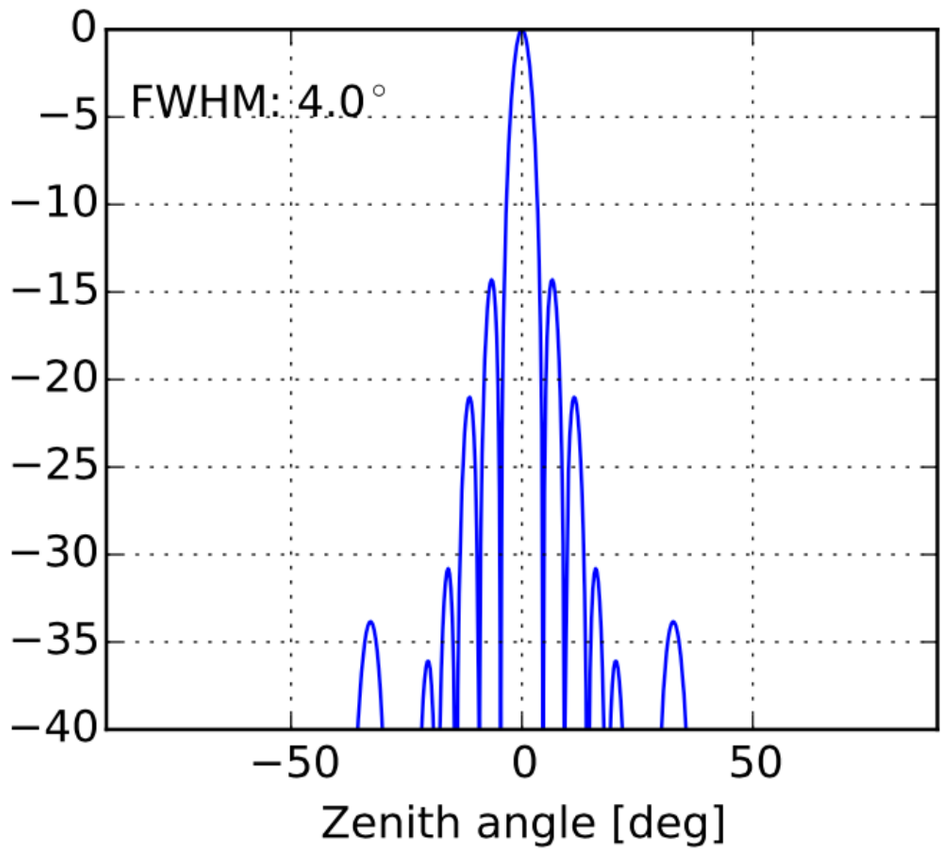

3.6 Next generation interferometers

- We can also combine different antenna receiver elements together coherently to form an aperture array (e.g. LOFAR; MWA; LWA).

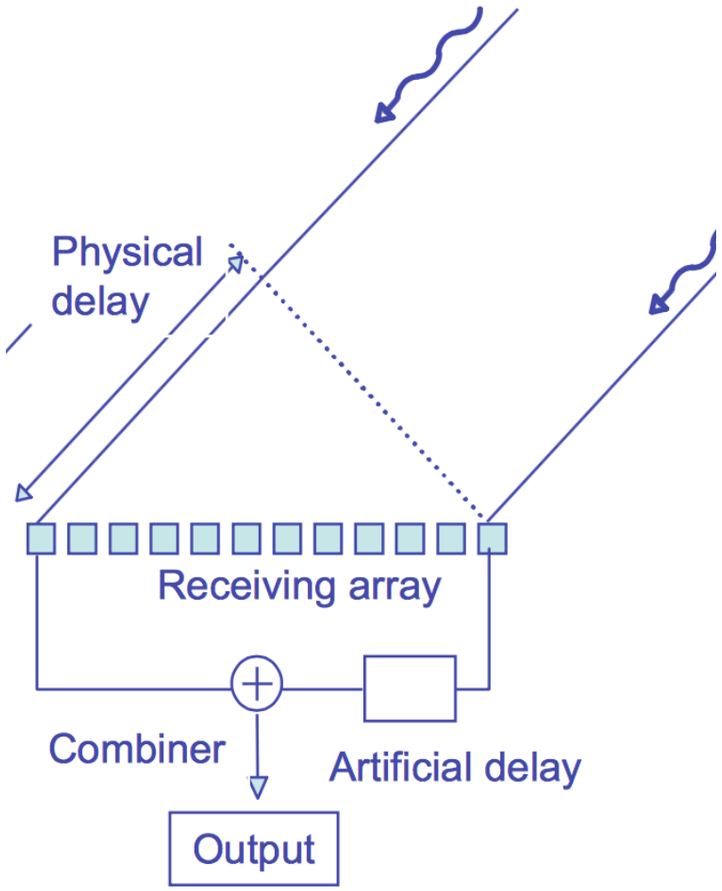

Tile **Station** **Core**

- Aperture array: In the same way that an interferometer works, the receiving elements are added together by taking into account the delay due to the waves arriving at different times, from different directions.
    1. Low cost (no moving parts, dipole elements).
    2. Better effective area at low radio frequencies.
    3. Large fields-of-view and flexible electronic beam forming.

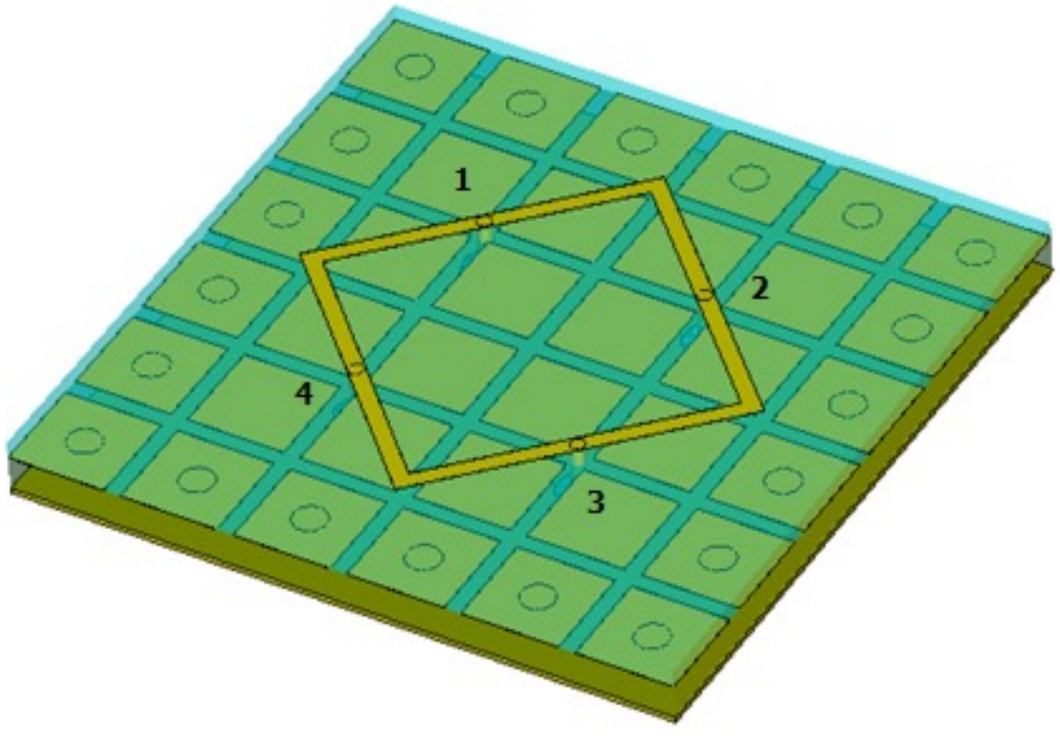
1
2
3
4

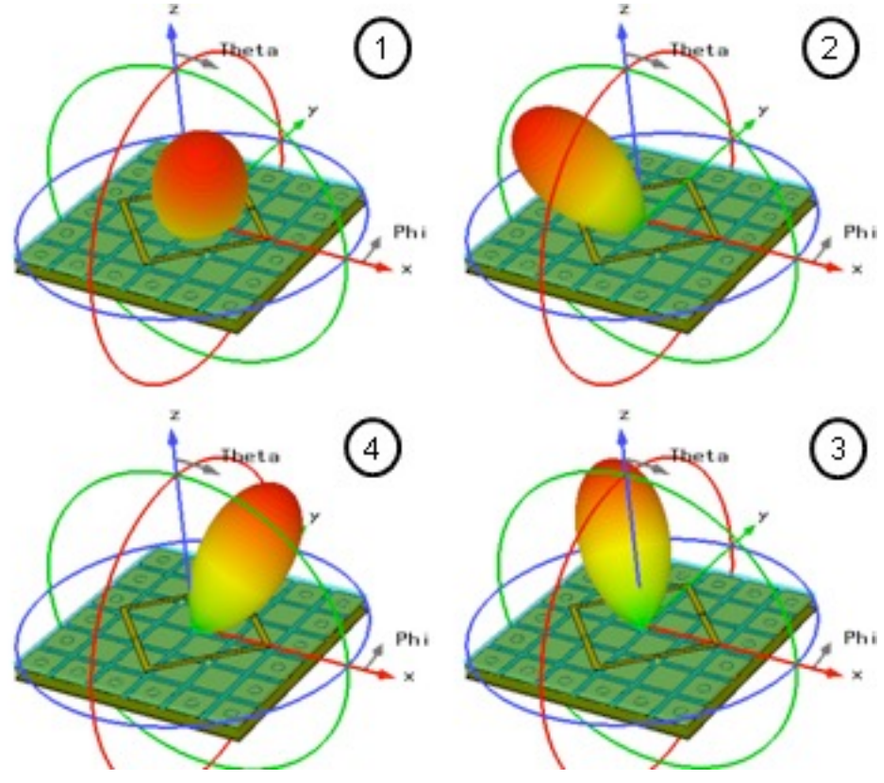
z
Theta
y
Phi
x
1
2
4
3

4.1 The Low Frequency Array

- International LOFAR Telescope being built by a consortium of institutes in the Netherlands, Germany, UK, France, Sweden, Poland and Ireland.

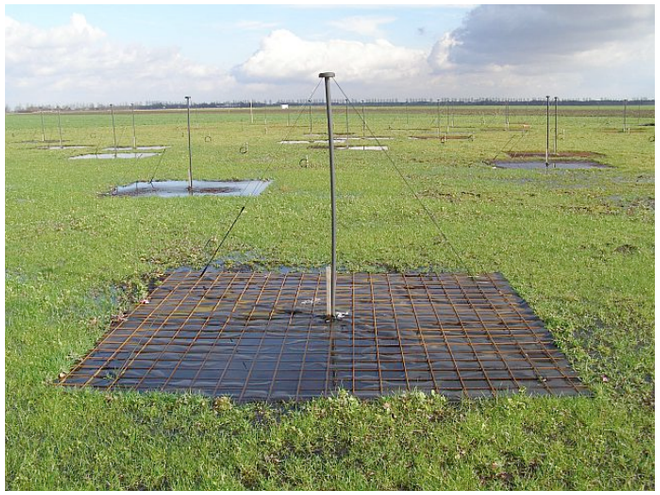

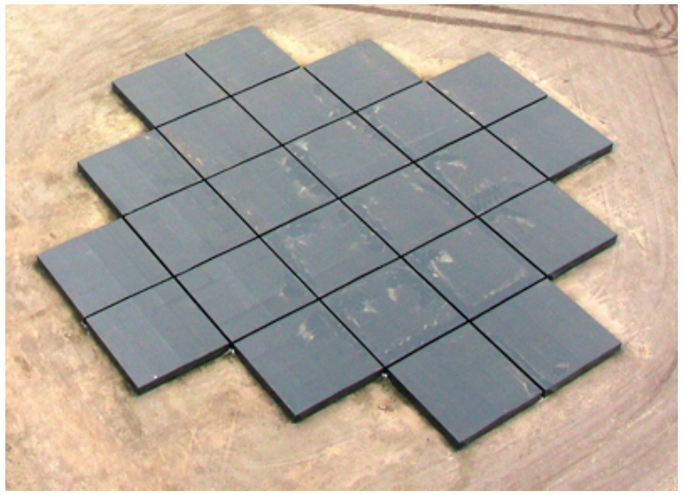

- Low Band Antenna (LBA; 10--90 MHz) - simple dipoles.
- High Band Antenna (110-180 MHz, 210-240 MHz) - tiled array.
- 96 MHz bandwidth.

- 50 Stations throughout Europe (~50 m to 1500 km baselines), resolution ~few degrees to sub-arcsec.

4.2 The Murchison Wide-Field Array

- Low frequency pathfinder based in Australia (quiet-site).

- 80--300 MHz frequency coverage, with 32 MHz instantaneous bandwidth.
- 128 tiles, with 4 x 4 dipoles (very like LOFAR).
- Max baseline to 3 km outriggers; most tiles (112) within 1.5 km.

- Wide field-of-view (15-45 degrees)
- Resolution of 2.5 to 8.5 arcmin

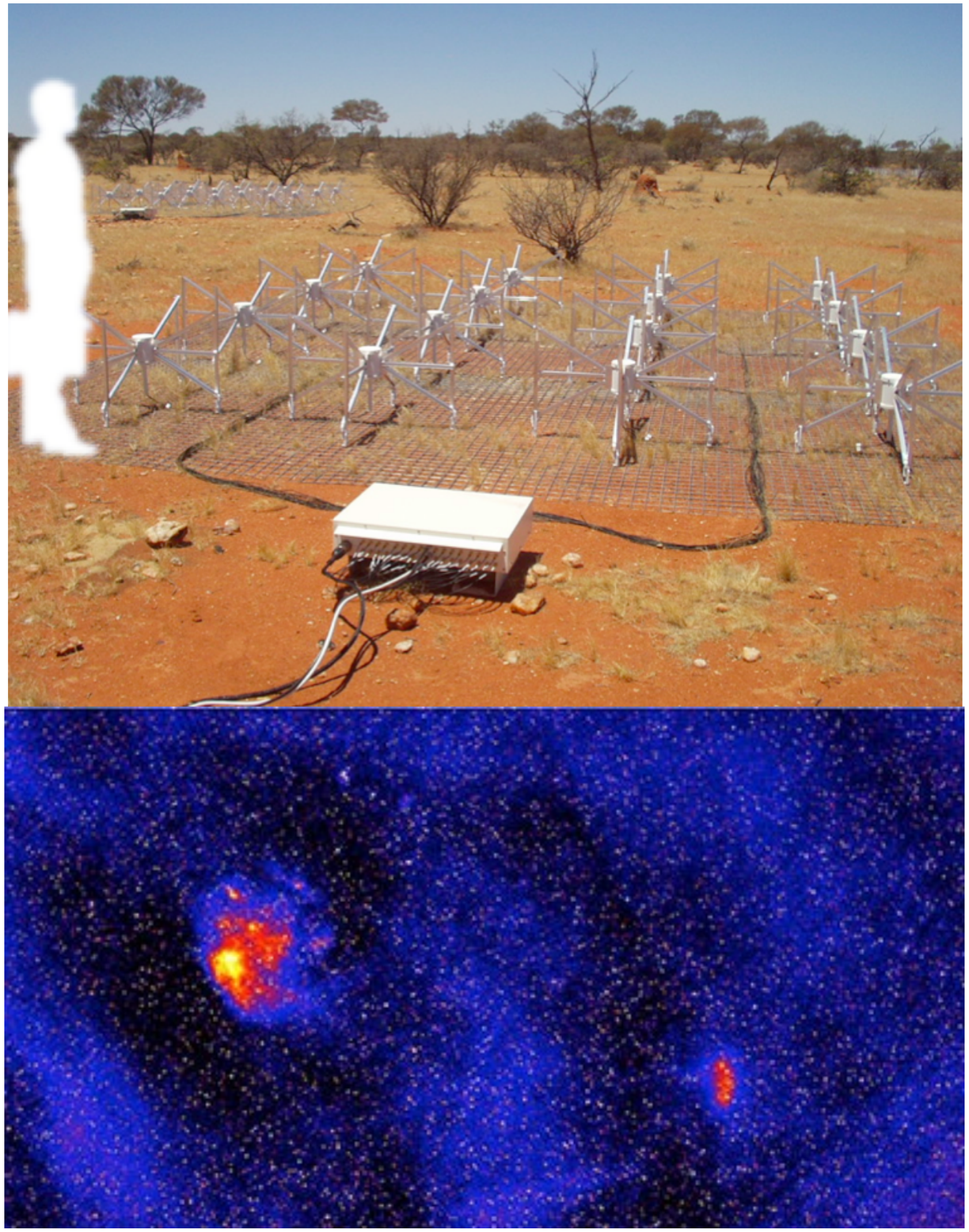

4.3 The Very Large Array

- Upgraded VLA, P-band (230-470 MHz).
- Receivers in place to sample down to 50 MHz.

- 27 x 25 m dish antennas with baselines up to 36 km in 4 configurations (A-D)

4.4 Long Wavelength Array

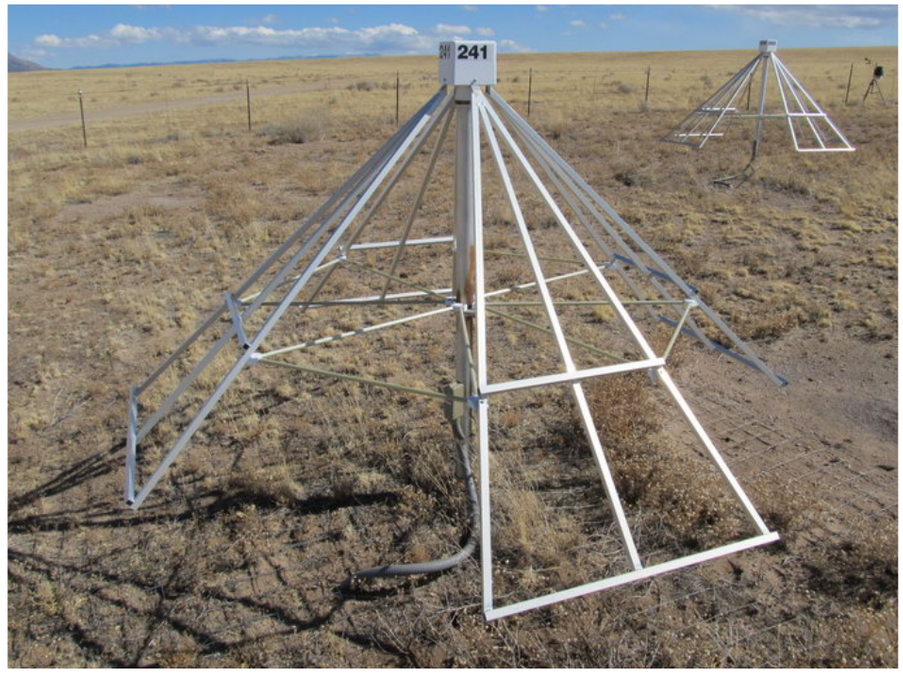

- 10-88 MHz; 4 simultaneous beam.
- LWA1 = 256 (+1) dual polarisation dipoles (100 x 110 m station)
- Full array; Ambitions to have baselines up to 400 km (~50 stations in NM; USA)
- LWA2 currently under construction (19 km baseline to LWA1)

4.5 Giant Metrewave Radio Telescope

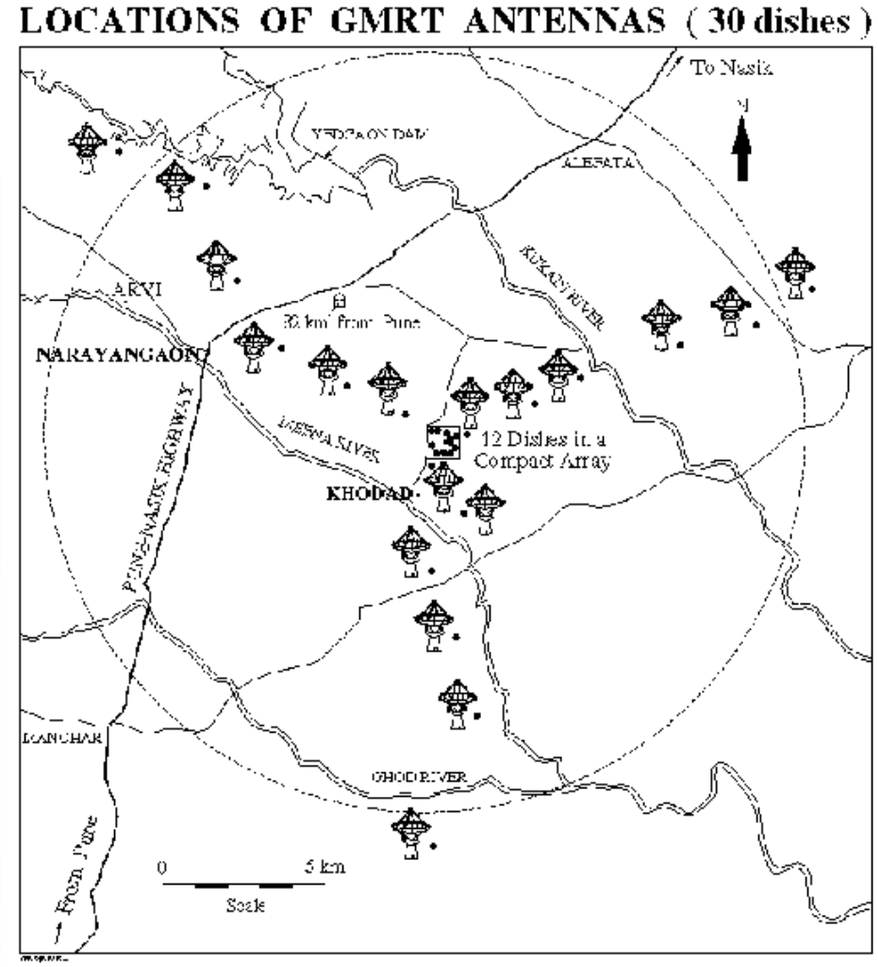

- Low frequency bands at 150, 235, 327 MHz (32 MHz bandwidth).
- 30 x 45 m antennas.
- Baselines up to 25 km
- Upgrade underway, providing contiguous 30-1500 MHz (400 MHz bandwidth).

4.6 Square Kilometre Array (SKA)

- Sparse dipoles (dual pol; similar to LOFAR).
- Freq: 50 to 350 MHz (300 MHz bandwidth).
- 130000 dipole antennas.
- 8 x more sensitive than LOFAR
- 50% collecting area at < 600 m, 75% at < 1 km.
- Spiral arms out to 50 km (100 km baselines), containing only ~4% of the collecting area.
- Dense core for EoR and Pulsar timing experiments (1 mK brightness temperature for 5 arcmin structures).
- $A_{eff} / T_{sys} \sim 1000\ m^2 / K$ (>100 MHz).

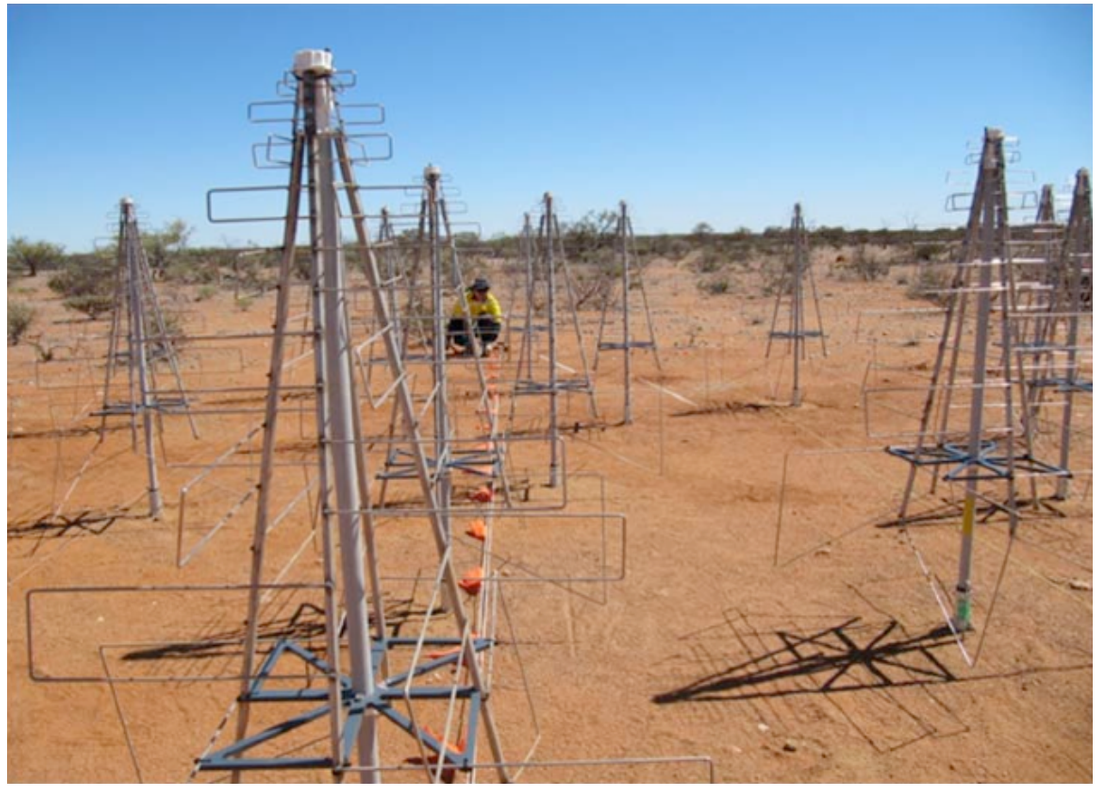

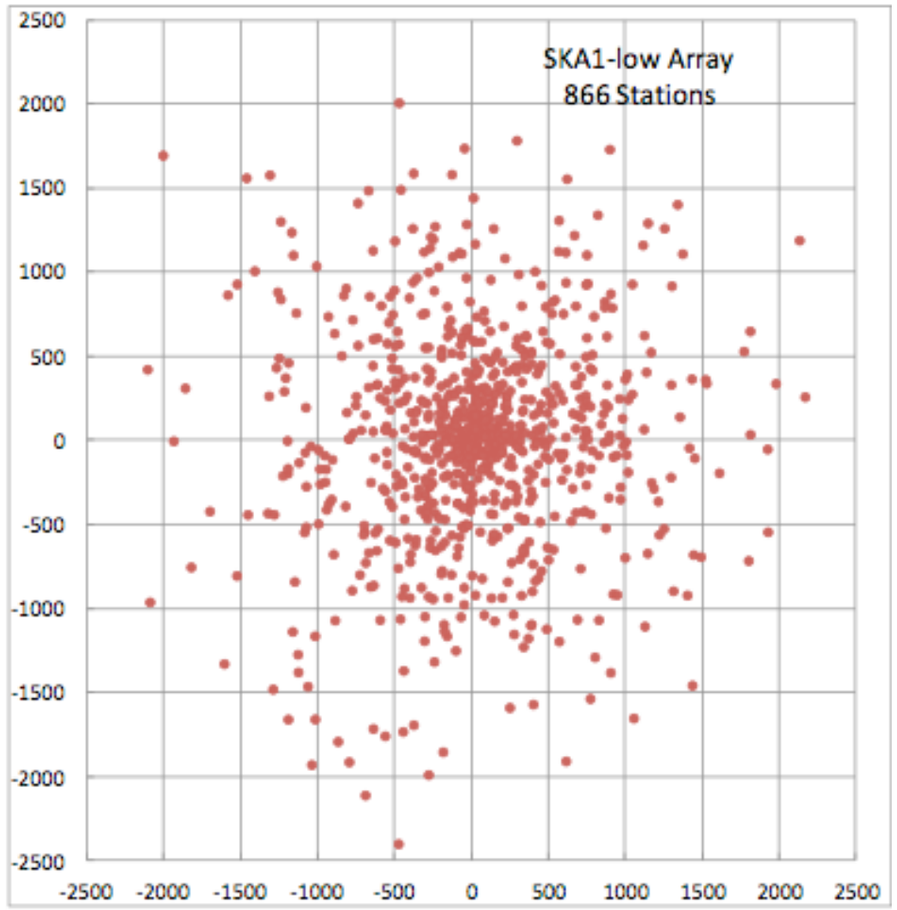

4.6 Square Kilometre Array (SKA)

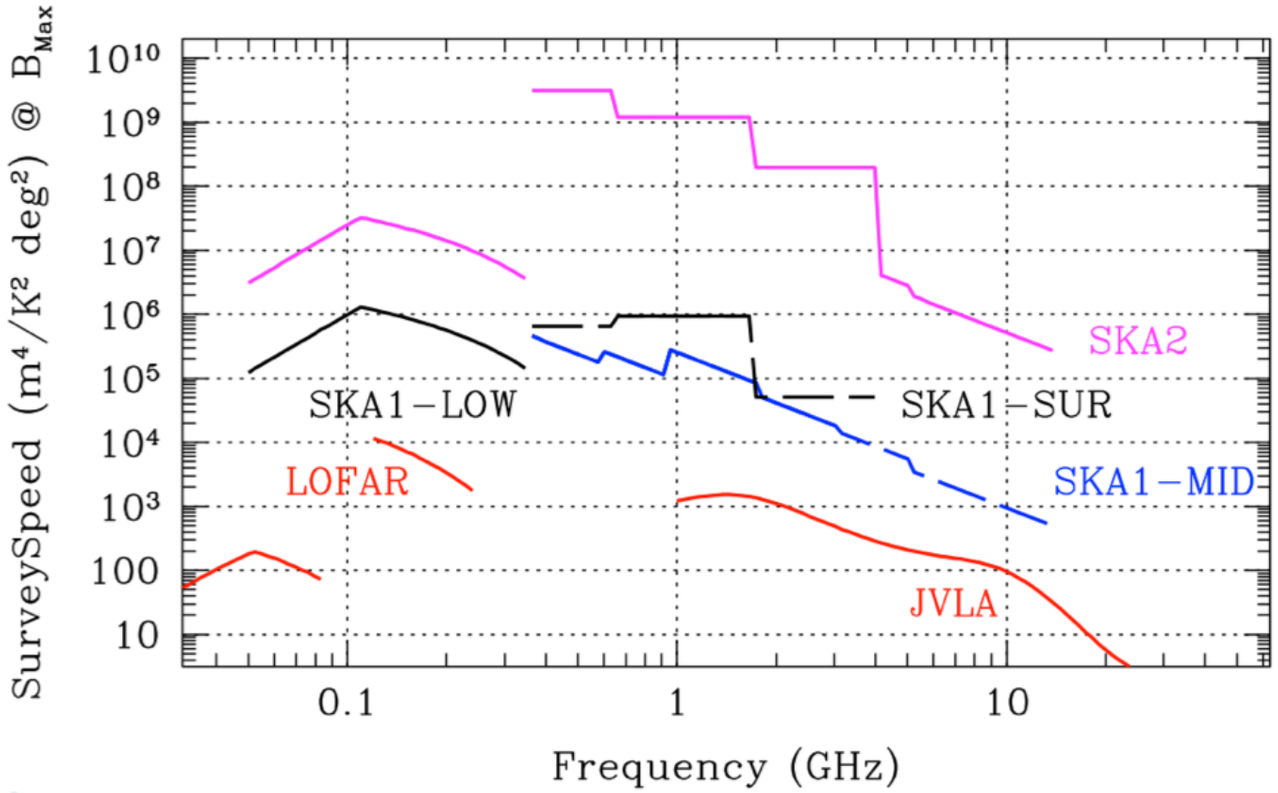

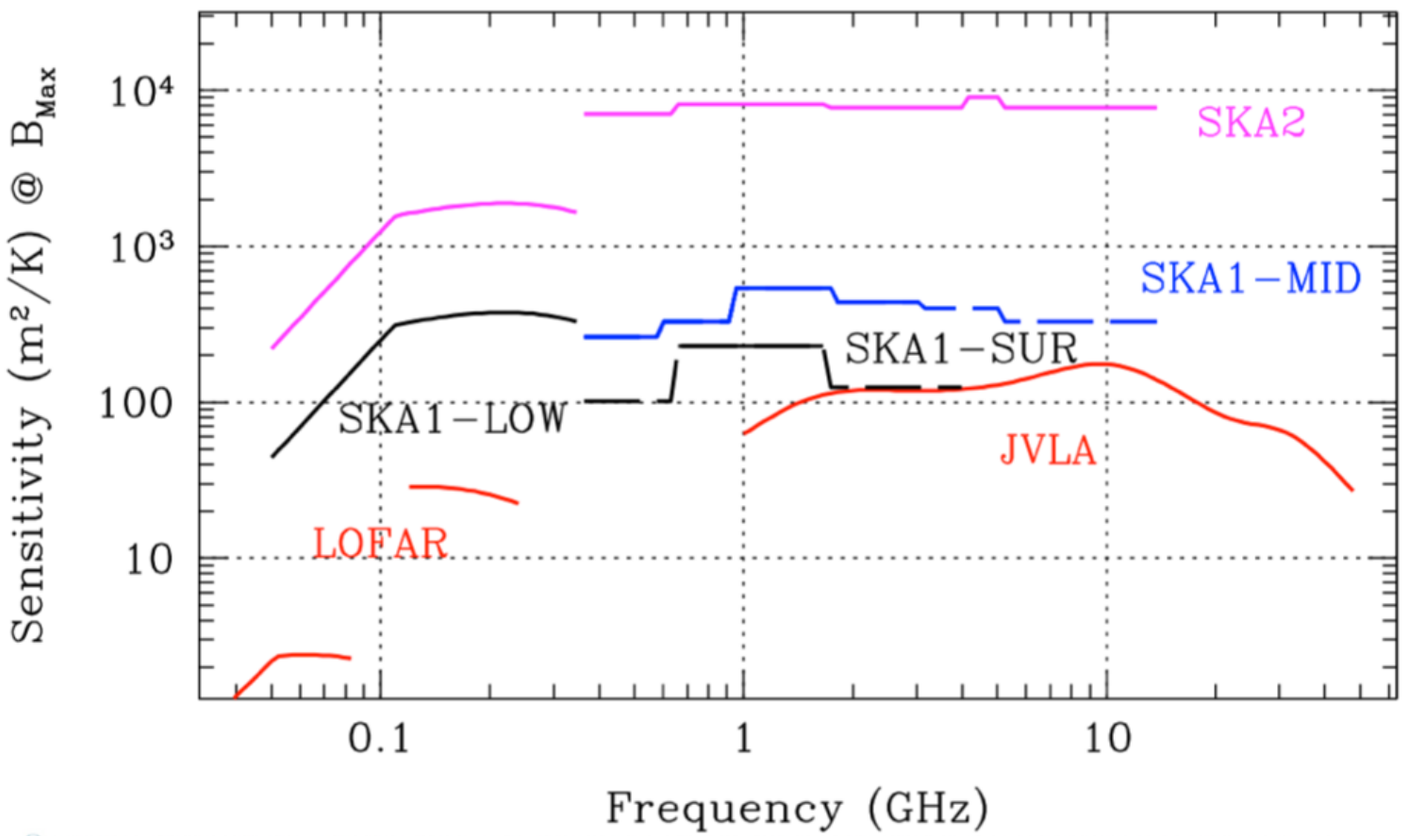

Summary

1. Radio astronomy had its origins at low frequencies, and after a successful diversion to higher frequencies, attention is returning to < 350 MHz.
   - Modern dipoles still quite simple (cheap, easily replaced, large fields-of-view, large effective collecting area).
   - Need large computing power for correlation and data processing (see lecture on LOFAR Overview).

2. Interferometry is essential for competitive low frequency science.
   - Increases angular resolution and sensitivity at cost to filtering structure on large angular-scales and complicating the point-spread function.
   - Requires detailed calibration (see lectures on Calibration, Error Analysis and Ionosphere) and special wide-field, wide-bandwidth imaging techniques (see lectures on Imaging).

3. Several important low frequency radio telescopes available (LOFAR, LWA, GMRT, VLA, MWA) and upcoming (SKA).